Study Report on Cooling Capacity of ACA Correlator Room for ACA Spectrometer

CORL-64.00.00.00-0013-A-REP

Version: A.2
Status: Draft
2019-10-13

Prepared by:	Organization:	Date:
Takashi NAKAMOTO	NAOJ	

Reviewed by:	Organization Role:	Date and Signature:
Jongsoo Kim	KASI ACA Spectrometer Principal Investigator	
Tetsuhiro MINAMIDANI	EA-ALMA ACA Spectrometer Project Manager	
Manabu Watanabe	NAOJ ACA Spectrometer Team Leader	

Released by:	Organization Role:	Date and Signature:
Tetsuhiro MINAMIDANI	EA-ALMA ACA Spectrometer Project Manager	

Change Record

Version	Date	Affected Section(s)	Author	Reason / Initiation / Remarks
A.0	2019-06-29	All	Takashi NAKAMOTO	Initial draft for internal team review.
A.1	2019-07-11	2.1.1 All	Takashi NAKAMOTO	Incorporated Jongsoo Kim's contribution about the GPU power consumption measurement in section 2.1.1. Assigned a number to each equation.
A.2	2019-10-13	1.3, 2.1.5	Takashi NAKAMOTO	Assigned ALMA documentation ID. Refer to a power supply efficiency test report made by an independent third-party test firm to explain the power loss. Reflected review comments from Manabu Watanabe. Added link to RD09.

Table of Contents

1 Introduction

KASI and NAOJ are jointly developing ACA Spectrometer for ALMA. We plan to install the new ACA Spectrometer in the ACA Correlator Room at AOS. The heat dissipation from the ACA Spectrometer is estimated to be 7.7 kW. This document shows the existing HVAC system for the ACA Correlator Room is capable of cooling the additional heat source. In addition, this document estimates how high the room temperature can be with the additional heat source, and shows that the estimated temperature increase is acceptable from the viewpoint of the ACA Correlator operation.

1.1 Scope

The purpose of this document is to show that the existing HVAC system is capable of cooling both ACA Correlator and ACA Spectrometer. This document starts with the thermal analysis (heat dissipation and air flow) of the ACA Spectrometer. Then, the current status of the ACA Correlator Room including the HVAC system is investigated referring to the existing documents and temperature measurement data. Thermal design of the ACA Correlator is also revisited to investigate the temperature margin and the actual air flow. Finally, combining all the findings above, this document shows that the exiting HVAC system is capable enough.

1.2 Applicable Document

The following documents are part of this document to the extent specified herein. If not explicitly stated otherwise, the latest issue of the document is valid.

No.	Document Title	ALMA Doc. Number
N/A	N/A	N/A

1.3 Reference Documents

The following documents are referenced within the present document to the extent specified herein. If not explicitly stated otherwise, the latest issue of the document is valid.

No.	Document Title	ALMA Doc. Number
RD01	Product Specifications: Intel Xeon Gold 6144 Processor	
RD02	PWS-2K05A-1R 2000W 1U Redundant Power Supply Specification	
RD03	(Product web page of PFR0912XHE-A01 (FAN-0151L4))	
RD04	Specification for Approval: PFR0912XHE-SP00	
RD05	(Product webpage of Fujitsu Server PRIMERGY RX1330 M4)	
RD06	(Data Sheet of Netgear GS750E)	
RD07	Interface Control Document between Site (AOS Technical Building) and ACA Correlator	ALMA-20.01.02.00-62.00.00.00-B-ICD

RD08	AOS Technical Building Design Development Package, 2004 April 13	SITE-20.01.02.00-0008-A-DWG
RD09	York Air Handling Unit Solution - Performance Specification AHU-6	(link in EDM)
RD10	Carrier Corporation, Product Data: 30GTN,GTR Air-Cooled Reciprocating Liquid Chillers with ComfortLink controls 50/60 Hz 1999	
RD11	Todd R. Hunter, Robert Lucas, Dominique Broguière, Ed B. Fomalont, William R. F. Dent, Neil Phillips, David Rabanus, Catherine Vlahakis, "Analysis of antenna position measurements and weather station network data during the ALMA long baseline campaign of 2015," Proc. SPIE 9914, Millimeter, Submillimeter, and Far-Infrared Detectors and Instrumentation for Astronomy VIII, 99142L (19 July 2016); doi: 10.1117/12.2232585	
RD12	ACA Correlator Thermal Analysis and Test Report, Revision H (2010.4.1)	NF-ACACOR-2006-0034
RD13	ACA Correlator ACA-CCC Protocol Plan	CORL-62.00.00.00-009-A-PLA
RD14	ALMA Environmental Specification	ALMA-80.05.02.00-001-B-SPE
RD15	ARX Group, Technical: Air Volume Calculation	
RD16	ARX Group, Technical: P&Q	
RD17	Nidec Servo Corporation, Technical Description of AC/DC Axial Fans and Blowers (Japanese) 日本電産サーボ株式会社、技術解説「AC・DC軸流ファン＆ブロア」	
RD18	Technical Investigation Report NCR-44 – "Power Socket burned of the ACA Correlator" and new design proposal	ALMA-20.01.02.07-0015-A-REP
RD19	Jingquan Cheng, Forced Air Cooling at High Altitude March 24, 1998	MMA Memo 203
RD20	80 PLUS Verification and Test Report for Super Micro Computer Inc. PWS-2K05A-1R	

1.4 Acronyms

The more complete list of acronyms and abbreviations used within this document are given below. For a complete set of acronyms and abbreviations, please go to the ALMA Acronym Finder web page.

ACA	Atacama Compact Array
AHU	Air Handling Unit
ALMA	Atacama Large Millimeter Array
AOS	Array Operation Site
AOSTB	Array Operations Site Technical Building

API	Application Programming Interface
ASC	ACA Spectrometer Controller
ASM	ACA Spectrometer Module
CFM	Cubic Feet per Minute
CHWS	Chilled Water Supply
CHWR	Chilled Water Return
CIP	Correlation Integration Processor
CPU	Central Processing Unit
DFP	Data Transmission System Receiver and FFT Processor
DRXP	DTS Receiver Board with PCIe Interface
DTS	Data Transmission System
EMCS	Energy Management Control System
FFT	Fast Fourier Transform
FPGA	Field Programmable Gate Array
GPU	Graphical Processing Unit
ICD	Interface Control Document
IF	Intermediate Frequency
IPMI	Intelligent Platform Management Interface
KASI	Korea Astronomy and Space Science Institute
MCI	Monitor & Control Interface
NAOJ	National Astronomical Observatory of Japan
HVAC	Heating Ventilation and Air Conditioning
PCIe	Peripheral Component Interconnect Express
TDP	Thermal Design Power
VAV	Variable Air Volume

2 Heat Dissipation from ACA Spectrometer

In this chapter, the heat dissipation from the ACA Spectrometer is estimated based on the power consumption estimation of all electrical devices. ACA Spectrometer consists of four ACA Spectrometer Modules (ASMs), one ACA Spectrometer Controller (ASC) and two network switches. Table 1 summarizes power consumption of those devices for the ACA Spectrometer. The ACA Spectrometer will consume **7.7 kW** in total. It is thought to be slightly overestimated because the power consumption of CPUs, GPUs, network switches and ASCs were estimated to be on the safe side as discussed in the following subsections. So, in this study, we assume that the heat dissipation is 7.7 kW to be on the safe side.

Table 1: Estimated power consumption of ACA Spectrometer

Device	Power Consumption	Qty	Subtotal
ASM	1.8 kW	4	7.2 kW
ASC	450 W	1	450 W
Network Switch	30 W	2	60 W
		Total	7.7 kW

Note that we plan to install one spare ASM and one spare ASC in the ACA Correlator Room as cold spare, but the power consumption of those spares is not taken into account because they will be off during the science operation.

The following sections estimate the power consumption of each device in detail.

2.1 Power Consumption of ASM

The main heat sources of the ACA Spectrometer are ASMs. An ASM is a commercial server with GPUs and Production DRXPs, which are custom-made PCIe boards to receive optical signals from the antennas. We selected Supermicro SYS4029GP-TRT as the base model of the ASM. One ASM has two CPUs (Intel Xeon Gold 6144), four GPUs (NVIDIA TITAN V), two Production DRXPs, four power supply modules (Supermicro PWS-2K05A-1R) and eight chassis fans (Delta PFR0912XHE-A01).

The power consumption of one ASM is estimated to be **1.8 kW** as summarized in Table 2. The following subsections discuss more details of the power consumption of each component in the ASM.

Table 2: Estimated power consumption of one ASM.

Component	Model	Power Consumption	Qty	Subtotal
CPU	Intel Xeon Gold 6144	150 W	2	300 W
GPU	NVIDIA TITAN V	200 W	4	800 W
Production DRXP		25 W	2	50 W
Chassis Fan	Delta PFR0912XHE-A01	54 W	8	432 W
Power Supply	Supermicro PWS-2K05A-1R	30 W	4	121 W
Overhead		59 W	1	59 W
			Total	1.8 kW

Figure 1: **Picture of Supermicro SYS4029GP-TRT, the base server model of ASM (https://www.supermicro.com/a_images/products/views/4029GP-TRT_angle.jpg). In this example picture eight GPUs are inserted to the PCIe slots. For ACA Spectrometer, only four GPUs and two Production DRXPs will be inserted instead.**

2.1.1 Power Consumption of GPU

We selected NVIDIA TITAN V for the GPUs of the ASM. TDP of TITAN V is 250 W. In reality, the GPU resources will not be fully used in our application.

To estimate the required power consumption, we designed a test setup to simulate a real observation of the ACA TP Array using a prototype ASM based on SYS4028GR-TRT, which is one generation ago machine of SYS4029GP-TRT. We generated 96 Gbps (3-bit x 4 Gsps x 2 pol x 4 antennas) signal in a CPU and continuously fed the signal into four GPUs; two TITAN X and two TITAN Xp. The

on-source and off-source times were 300 seconds and 30 seconds, respectively. The off-source time was to mimic, for example, slewing time of the antennas of the TP Array. The on- and off-source observations were repeated 20 times. The total number of spectral channels which covers a 2 GHz bandwidth was 4096. The GPU calculated (1) bit conversion from 3-bit to 32-bit float, (2) 220 point FFTs for each polarization, (3) accumulation of auto-power spectra, and (4) spectral averaging to reduce from 219 to 4096 channels. TITAN X and TITAN Xp consumed 116.1 W and 105.7 W, respectively, per GPU on average during the test. Figure 2 shows trend of the power consumption of the two GPUs during the test. Because the ratio of the on-source time was 91%, the average power consumption during on-source time was estimated to be 128 and 116 W respectively.

Although we have used older generation GPUs than TITAN V, we expect that one TITAN V on the ASMs is expected to consume around 116 W on average. Because, in general, TITAN V has better performance v.s. power consumption ratio than TITAN X and TITAN Xp, the expected power consumption can be lower than 116 W. In contrast, the test program does not include some minor required calculations like frequency profile synthesis, residual delay correction and cross-antenna correlation, so the actual power consumption can be a bit larger than the measured result in this sense. So, all in all, what we can say now is that, the average power consumption of one GPU will be around 116 W. In this study, we assume that one GPU consumes 200 W to be on the safe side to accommodate any overlooked required calculations and/or future extensions.
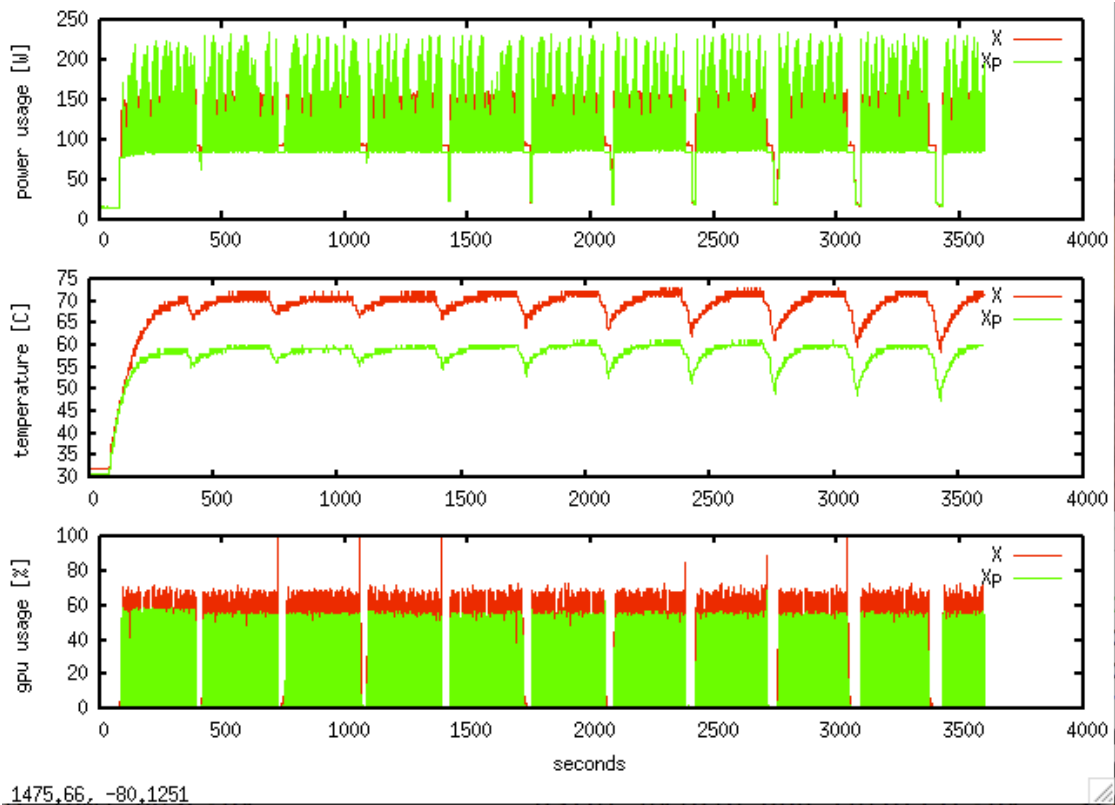
Figure 2: **Trends of GPU power consumption, temperature and GPU utility of TITAN X and TITAN Xp during a power consumption measurement test.**

2.1.2 Power Consumption of CPUs

One ASM has two CPUs, Intel Xeon Gold 6144. TDP of one CPU is 150 W [RD01]. We currently do not know how much power the CPUs will use. All calculation that needs a lot of computation resources including FFT, correlation, accumulation and binning will be performed in GPUs, not CPUs. So, in principle, the power consumption of the CPUs is thought to be limited. However, to maximize the responsiveness to the time critical tasks (e.g. memory copy from a DRXP ring buffer to GPUs when an interruption from DRXP is asserted), the scaling governor of the CPUs may be set to "performance" which sets the CPU frequency maximum all the time. With that scaling governor, the total power consumption of the two CPUs are approximately 70 W in an idle state according to the output of `powerstat -R -c -z` command. It is almost the quarter of the total TDP (300 W). Moreover, it is difficult to estimate the total CPU power consumption at the time of writing when the software implementation is not completed. It may use a lot of computation resources for housekeeping tasks. Thus, in this study, it is assumed that the two CPUs will consume the same amount of TDP (300 W) in total during the science operation to be on the safe side.

2.1.3 Power Consumption of Production DRXPs

One ASM comes with two Production DRXPs, which is a custom-made PCIe board to receive optical signals from the antennas. The device driver for Production DRXPs provides an API to retrieve the current power consumption of the board. According to a measurement using that API, Production DRXP typically consumes 25 W when receiving two IF signals (six optical signals in total). So, in total, the two Production DRXPs consume 50 W.

2.1.4 Power Consumption of Chassis Fans

The ASM comes with eight chassis fans Delta PFR0912XHE-A01. The maximum input power of one unit is 54 W (see Appendix A for more details). As of writing this report, we have not determined how to control the chassis fans. There are currently three choices: (1) set the fan speed to full all the time, (2) use "Heavy IO" mode for optimal fan speed of the PCIe cards and (3) make our own software to effectively control the fan speeds. We have not currently investigated option (2) and (3) yet and the safe choice as of writing this document is (1) in order to cool the GPUs below the acceptable temperature threshold where the GPU clock frequency is automatically decreased. Therefore, in this study, we assume that the fan speed is always full, and each chassis fan consumes the maximum input power 54 W, which results in 432 W in total in one ASM.

2.1.5 Power Loss at Power Supplies and Others

The ASM has four power supply modules, Supermicro PWS-2K05A-1R. One power supply module can provide 2000W and it has 80 Plus Titanium efficiency [RD02]. The IPMI interface of SYS4029GP-TRT allows us to monitor the input and output power of each power supply module.

To simulate the power consumption during the science operation, we ran `stress -c 32` command to make the two CPUs (eight cores for each) consume 300 W in total, ran `gpu-burn` command to make the four GPUs consume 800 W in total, ran a DRXP test program to make Production DRXPs consume full power and set the chassis fan mode to "Full" so that the chassis fans consume the maximum power. The actual power consumption of CPUs, GPUs and Production DRXPs were measured using dedicated APIs or commands. The two CPUs consumed 300 W, the four GPUs consumed 796 W in total and Production DRXPs consumed 49 W in total. In that condition, the difference between the input and output power of all four power supply modules were 121 W in total while the total input power was 1757 W (22% load out of full capacity). It means that 6.9 % of the input power was lost in the power supply modules. This result is almost consistent with the tests conducted by a third-party independent test firm, which confirmed 95% efficiency (5% loss) at 20% load [RD20].
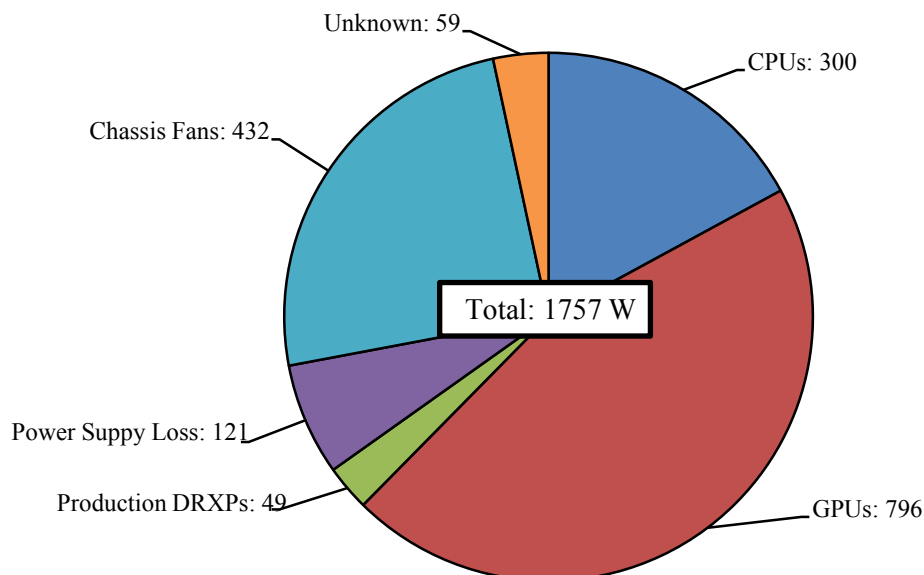
Figure 3: Breakdown of the power consumption of one ASM. The power consumption of two CPUs, four GPUs and two Production DRXPs were actually measured using APIs and/or commands. Power supply loss was the difference between the output and input of the power which can be obtained through the IPMI interface. The power consumption of the eight chassis fans were the total of the maximum input power supply in the specification. The total power consumption, 1757 W, was the sum of the input power of all the power supplies which can be obtained through the IPMI interface. The values in this chart is average power consumption in watt of approximately 5 minutes at a steady state.

If the eight chassis fans were assumed to be consuming the maximum input power (432 W in total), 59 W was consumed somewhere in the ASM. It is not exactly known which components in the ASM consume such power, but they may include the motherboards and memories.

2.1.6 Air Flow of ASM

As already explained, the base server (SYS4029GP-TRT) of the ASM has eight chassis fans. They are located on the front side of the chassis. Two fans in series form one set, and there are four sets in parallel as can be seen in Figure 4. Because maximum air flow of one fan is 185.7 CFM (5.26 m^3/min) according to RD03, the maximum total air flow of one ASM is 5.26 × 4 = 21.04 m^3/min. See Appendix C for more details why not multiplied by 8, but 4.
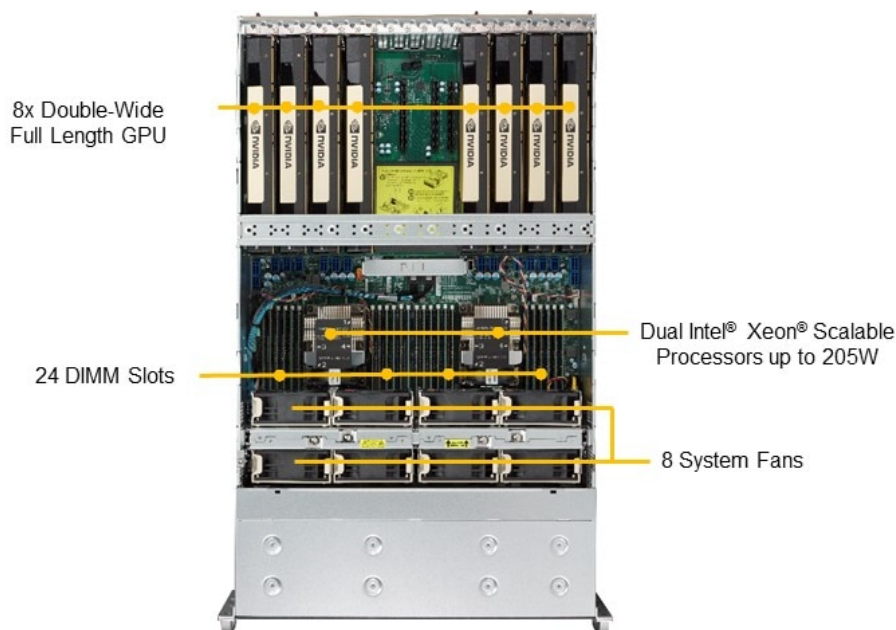
Figure 4: Top view of Supermicro SYS4029GP-TRT, the base server model of ASM (https://www.supermicro.com/a_images/products/views/4029GP-TRT_top.jpg).

Each chassis fan has a sensor to read the current rotation speed, which can be read though IPMI. We measured the actual fan rotation speed at ground level (Mitaka campus in NAOJ), OSF and AOS using a prototype ASM which consists of the following components:

- Supermicro SYS4028GR-TRT (one generation ago model of SYS4029GP-TRT)
- Delta PFR0912XHE-A01 × 8 (the same chassis fans as SYS4029GP-TRT)
- Prototype DRXP × 2
- TITAN X × 2 (two generation ago model of TITAN V)
- TITAN Xp × 2 (one generation ago model of TITAN V)

The measurement result is shown in Table 3. Note that the fan mode was set to "Full". The maximum rotation speed of the fan is 11500 RPM [RD03] ± 10% [RD04] according to the specifications. The measurement result at ground level meets the specification well. However, the higher the machine is located, the faster the fans rotate. At AOS, the fan speed is approximately 15 % faster than at ground level. It is possibly because the fan speed may be controlled to consume a constant power. According to RD19, by increasing the fan speed 22% at a 5,000 m altitude, the horsepower required from the fan motor remains constant assuming the fan motor does not have efficiency loss. In any case, the measurement indicates that the actual air flow (air volume flow rate, not air mass flow rate) can be larger than the specification for the ground level.

Table 3: Chassis fan rotation speed at ground level, OSF and AOS.

	Ground level (Mitaka)	OSF	AOS
Fan #1	11000 RPM	11700 RPM	12461 RPM
Fan #2	10902 RPM	11700 RPM	12500 RPM
Fan #3	10700 RPM	11600 RPM	12400 RPM
Fan #4	10389 RPM	11100 RPM	12786 RPM
Fan #5	11800 RPM	12800 RPM	13596 RPM
Fan #6	11900 RPM	12890 RPM	13700 RPM
Fan #7	11736 RPM	12700 RPM	13500 RPM
Fan #8	11900 RPM	12900 RPM	13799 RPM
Average	**11291 RPM**	**12174 RPM**	**12968 RPM**

Note that, the actual fan speed may not represent the flow rate we are interested in. In principle, air flow is proportional to fan speed. However, the air flow generated by the fan may include both the air taken in from the outside of the chassis and the one circulates within the chassis. What we are interested in is the air which the chassis takes in from the outside because the air circulating in the chassis does not contribute to cooling. Figure 5 describes that situation. Q is the flow rate of the air which the chassis takes in from the outside, $Q_{circulate}$ is the flow rate of the air which is circulating within the chassis and Q_{total} is the flow rate generated by the fans. Here, Q_{total} is proportional to the fan speed.

We actually measured the fan speed in two cases: (1) when an ASM is placed in open place (2) when the front panel is completely covered by papers as shown in Figure 6. When the front panel was not covered, the average fan speed of the eight chassis fans was 11475 RPM. When it was covered by the papers, the average fan speed was 11163 RPM. The fan speed only drops by 3 % even though the front panel was completely covered by the papers. It indicates that the fan speed does not directly reflect the flow rate of the air which the chassis takes in from the outside.
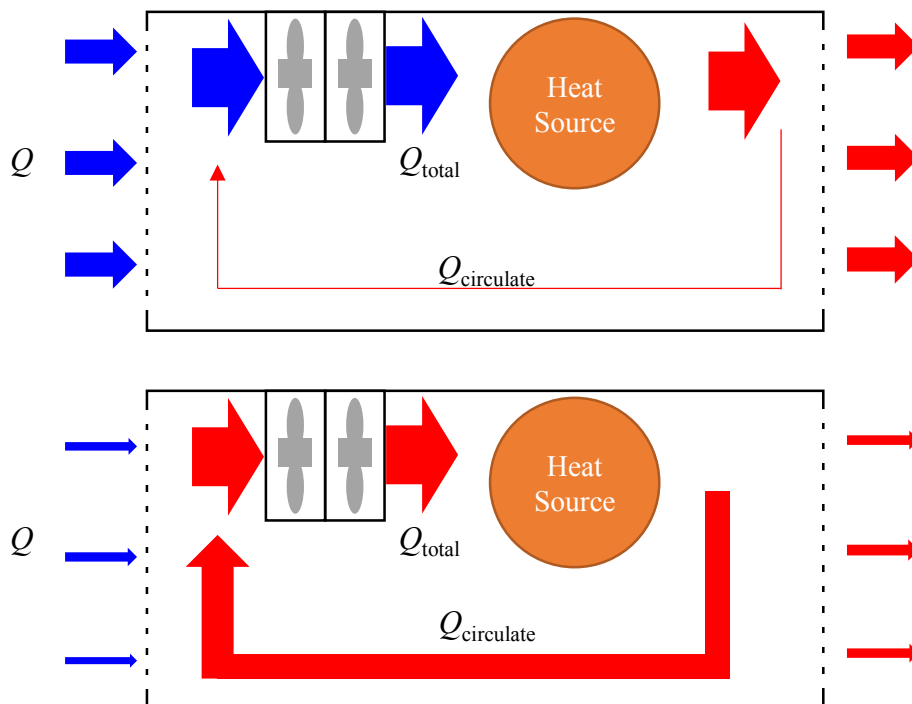
Figure 5: Schematics of possible air flow of the server chassis. In the upper case, the amount of the air circulating within the chassis is very limited. In the lower case, the inlet air is blocked for reasons and the fan is mostly circulating hot air within the chassis.

Figure 6: An ASM is located in open place, which is actually mounted in a 19inch rack (left), and the front panel is covered by papers to block cold air from coming in (right).

Instead of estimating the air flow of ASM from the fan speed, the author tried to estimate it from the temperature of the inlet air and the exhaust air when the ASM is consuming 1.8 kW. As a result of a quick measurement at ground level (Mitaka), it was found that the exhaust air temperature largely depends on where the temperature sensor is located. The highest temperature was recorded at behind a certain TITAN V, which was 43 ℃ while the inlet air temperature was 23 ℃. It was quite difficult to estimate average temperature of the exhaust air due to the locality, but the upper boundary of the temperature difference between inlet and exhaust air temperature is now determined as 43 – 23 = 20

°C. From this result, we can calculate the lower boundary of the air flow of the ASM. The relation between the air flow and the temperature difference is

$$Q_{\mathrm{ASM}} = \frac{q_{\mathrm{ASM}}}{\rho_0 C_p \Delta T_{\mathrm{ASM}}} \tag{1}$$

where q_{ASM} is the heat dissipation of the ASM in watt, ρ_0 is the air density in kg/m^3 at ground level, C_p is specific heat of the air (see Appendix A for more details) and ΔT_{ASM} is the temperature difference between the inlet and exhaust air temperature. Because ρ_0 = 1.3 kg/m^3, q_{ASM} = 1.8 kW and $\Delta T_{\mathrm{ASM}} \leq 20$ °C,

$$Q_{\mathrm{ASM}} > 0.069 \ \mathrm{m^3/s} = 4.1 \ \mathrm{m^3/min} \tag{2}$$

In reality, the air flow at AOS must be much larger than 4.1 m^3/min largely because the average exhaust air temperature must be lower than 43 °C. In addition, the air flow should be larger at AOS than at ground level.

2.2 Power Consumption of ASC

We selected Fujitsu PRIMERGY RX1330 M4 as the ASC [RD05]. It comes with two 450W power supplies. There are two power supplies for redundancy, so the power consumption will not exceed 450 W. The actual power consumption will be much less than 450 W, but here we assume one ASC server consumes and dissipates 450 W to be on the safe side.

Figure 7: Picture of Fujitsu PRIMERGY RX1330 M4
(https://jp.fujitsu.com/platform/server/primergy/products/lineup/rx1330m4/rx1330m4_catalog.pdf)

2.3 Power Consumption of Network Switch

Netgear GS750E was selected as the network switches for the ACA Spectrometer. One unit of GS750E consumes 30W in the worst case where all ports are used [RD06]. We plan to install two network switches, so the total power consumption (= heat dissipation) is 60 W.

Figure 8: Picture of Netgear GS750E
(https://www.netgear.jp/supportInfo/NewsList/382.html)

3 Current Status of ACA Correlator Room

This chapter shortly describels the current status of the ACA Correlator Room, before installing the ACA Spectrometer, mainly based on the existing ALMA documents.

3.1   ACA Correlator Room

The major heat sources in the ACA Correlator Room are ACA Correlator and associated computers. Those electrical devices are housed in racks in the room. The right picture of Figure 9 shows the room layout. The ACA Correlator are housed in ACA Corr. Set #0 – 3 racks while the computers and other equipment are housed in COMP. Set #0 – 3. As in typical server rooms, cold air from a HVAC system comes out from the floor of the center cold aisle. Then, the cold air goes through the electrical devices from the front side to the rear side of the racks. The hot air from the rear side of the racks finally returns to the ceiling.
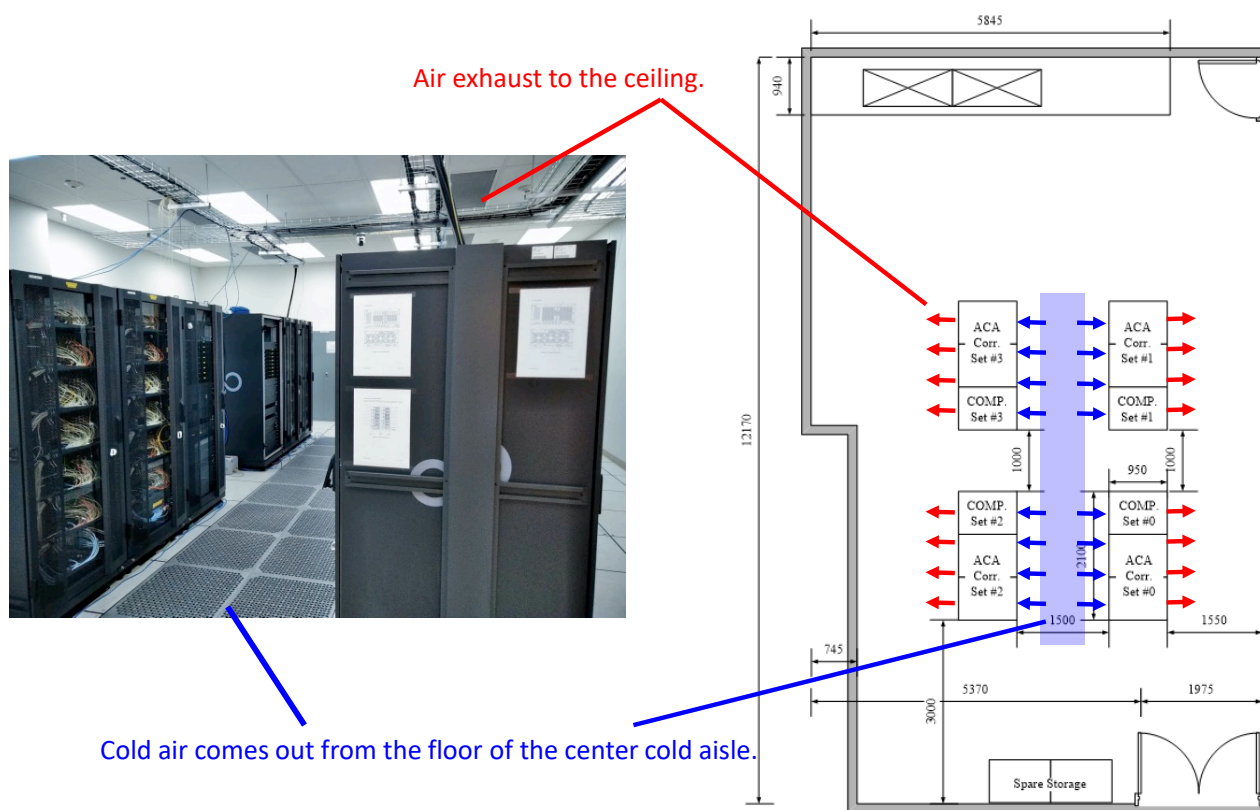
Figure 9:   Air flow in the ACA Correlator Room. Air comes out from the center cold aisle, goes through the electrical devices in the racks and finally returns to the ceiling. The room layout in the right figure is quoted from RD07.

Figure 10: Closer look at the floor of the center cold aisle where the cold air comes out (left) and at the ceiling where the hot air returns to (right).

Maximum heat dissipation from the ACA Correlator in the ACA Corr #0 – 3 racks is 65 kW while the ACA Correlator Computers and other electrical devices in the COMP Set #0 – 3 racks is 12 kW according to RD07. Thus, the maximum total heat dissipation in the ACA Correlator room is 77 kW.

3.2 AHU #6

The cold air in Room Correlator 2 (a.k.a. ACA Correlator Room) is provided by AHU #6 according to "AOS Tech Bldg Mechanical Hydronic Piping Mechanical Room" (SITE-20.01.02.05-007-A-DWG, page 27 of RD08).
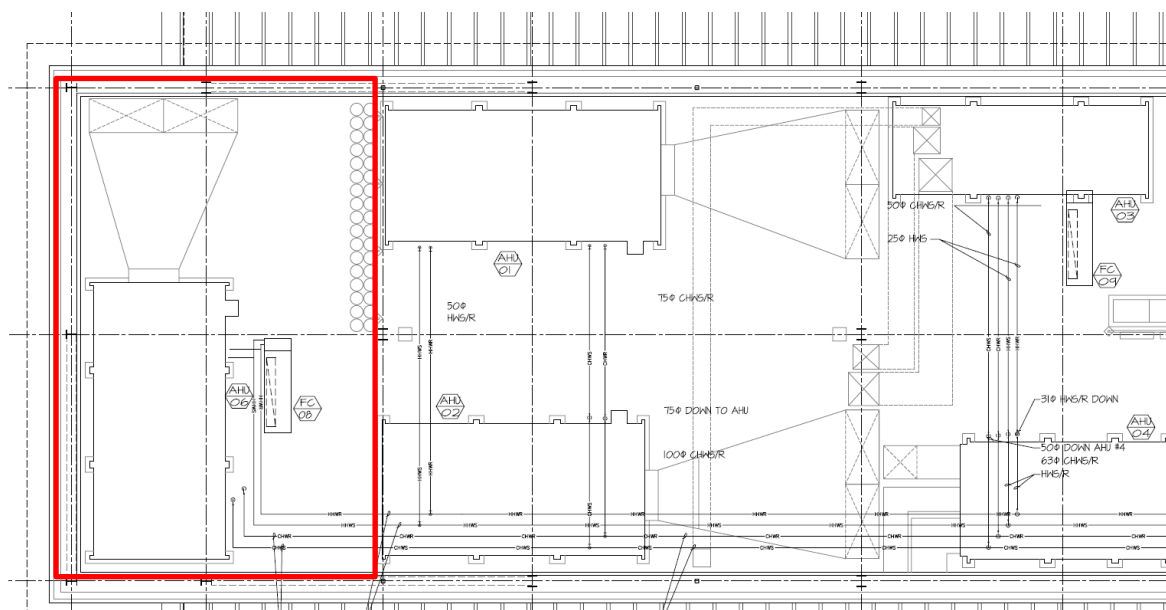
Figure 11: Excerpt from "AOS Tech Bldg Mechanical Hydronic Piping Mechanical Room" (SITE-20.01.02.05-007-A-DWG). This drawing shows air handling units located in the second floor of the AOSTB. The location of the ACA Correlator Room (Room Correlator 2) is emphasized with the red rectangular, in which you can find AHU #6.

According to "AOS Tech Bldg Air Flow Schematic" (SITE-20.01.02.05-005-A-DWG, page 25 of RD08, Figure 12), a typical AHU takes in hot air from a room, which is cooled by a cooling coil and supplies the cooled air to the room. To the cooling coil, chilled water is supplied for each AHU. Flow rate of the chilled water is adjusted by a valve which is controlled by Energy Management Control System (EMCS). The same document does not include the details of this control system, but it is thought to control the valve based on room temperature measured by a temperature sensor.

Figure 12 indicates that a typical AHU also takes in outside air and mix it with the air that is returned from the room. The amount of the outside air is controlled by the EMCS. Although RD08 only explains a "typical" AHU, another document RD09 explains more detail of AHU #6, which confirms that the unit sequence is as describe above (Figure 13). However, the author cannot find how the flow rate or the room temperature is controlled, or the amount of the outside air is controlled in AHU #6.

Figure 12 indicates that a typical AHU has a VAV box, which changes air flow to keep the room temperature constant. The author does not know whether this VAV box is applied to AHU #6. At least, such information cannot be found in RD09.

Maximum air flow of AHU #6 is 24029 CFM (680 m^3/min) at an altitude of 16505 ft (5030 m) according to RD09. Due to system impedance of the room (= flow resistance), the actual air flow must be lower than it, but we have not measured it in the past.
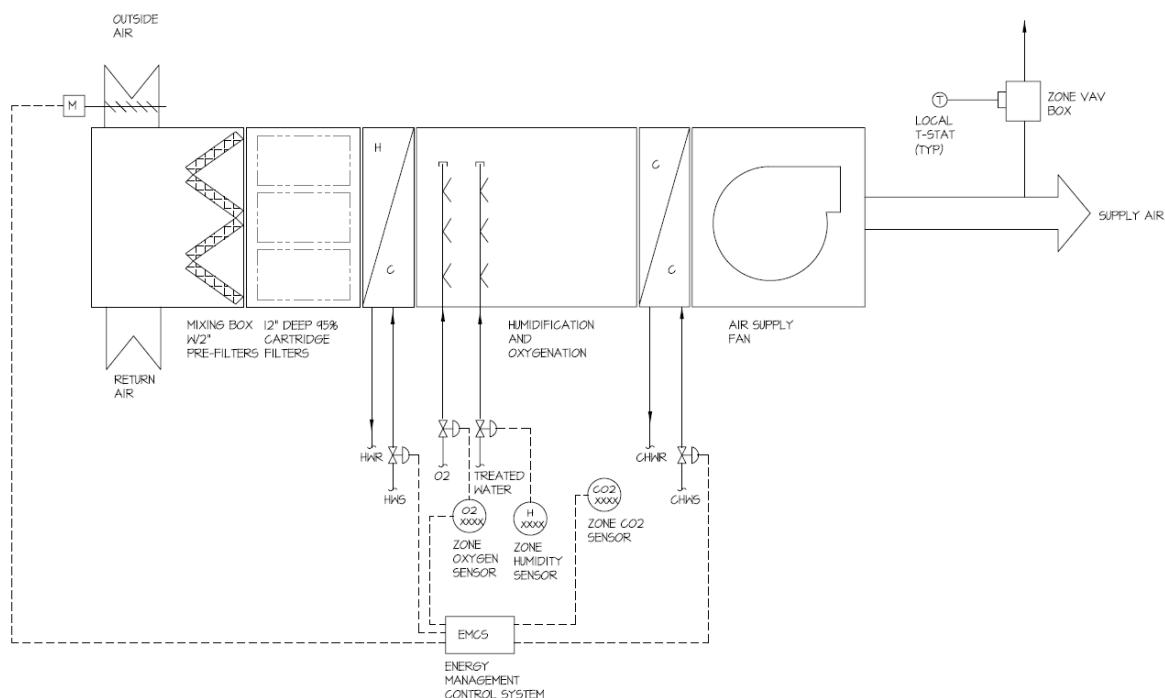
Figure 12: Schematic of a typical AHU. This is an excerpt from "AOS Tech Bldg Air Flow Schematic" (SITE-20.01.02.05-005-A-DWG).

SOLUTION AIR HANDLING UNIT PERFORMANCE SPECIFICATION

Unit Tag	Qty	Model	Air Flow (CFM)
AHU-6	1	Solution Indoor Air Handler 75 x 120	24029

Unit Sequence

Tier 1 [ ] [ ] [ ] [FS] <<< [RF] <<< [CC] <<< [XA] <<< [XA] <<< [HC] <<< [FM]

*This unit will not be used for 100% OA application

Basic Unit Options

Insulation Type: (Refer to Each Segment)   Exterior Casing Paint
Isolation Type: 1" Spring
Base Rail Height: 8"
*Note: Component locations are listed as Segment Hand (Unit Hand) : ex. Left (Right)
   See Submittal Drawing for additional details

Segments Listed Starting At Air Inlet

Figure 13: Top page of RD09. As can be found in the same document, the meaning of two letter abbreviations are following: FM – Filter/Mixing Box Segment, HC – Heating Coil Segment, XA – Access Segment, CC – Cooling Coil Segment, RF – High Efficiency Filter Segment, FS – Supply Fan Segment.
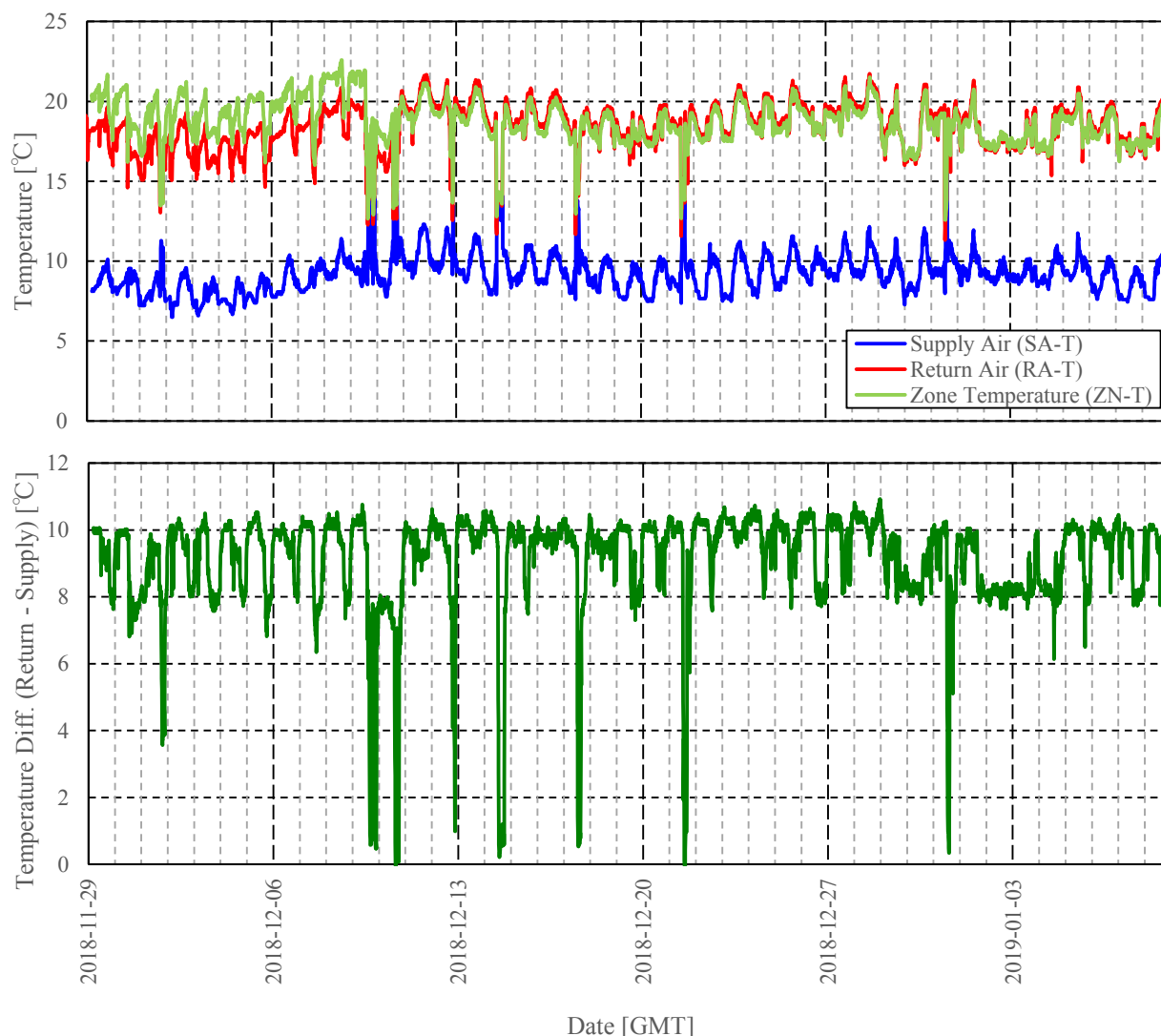
Figure 14: Trend of supply air temperature, return air temperature and zone temperature of AHU #6 between November 29th 2018 and January 9th 2019 (top), and trend of temperature difference between supply air and return air (bottom). Data source can be found in an e-mail from Tetsuhiro MINAMIDANI sent to alma-gpu@alma.mtk.nao.ac.jp on 2019-01-16 15:40 JST, which was originally provided by JAO.

Figure 14 shows trend of supply air temperature, return air temperature, zone temperature and temperature difference between supply air and return air of AHU #6 in December 2018 (+ α). The return air temperature sometimes drops below 15 ℃ and the supply air temperature goes up at the same time. In such case, the temperature difference is close to zero, which indicates that there is almost no heat dissipation in the room. It is thought that the operation of the ACA Correlator was suspended and powered off for some reason at that time. Except such suspended periods, the trend of the supply air temperature goes up and down every day and the maximum supply air temperature was 12.3 ℃ in December 2018. The daily cycles are thought to reflect a daily trend of outdoor temperature. As can be seen in Figure 15 and Figure 16, the supply air goes up when the outdoor temperature goes up. It is most probably because performance of chillers, which will be explained in section 3.3, is worse at higher temperature.

As can be seen in Figure 14, the temperature difference is typically between 8 and 10 °C and it seems to have daily cycles. When at the top flat of the daily cycles, the temperature difference is typically 10 °C. We do not exactly know why the trend of the temperature difference has such daily cycles at a glance. The author originally thought that it has something to do with the outdoor temperature, but it is not true all the time. For example, the temperature difference is almost constant whole day on December 16th 2018 (Figure 18). There are some possibilities like

- Observations did not use the ACA Correlator. If no subarray is created on the ACA Correlator, the power consumption of the ACA Correlator and the associated computers may drop, hence the temperature difference drops.
- Air flow is controlled with a certain logic in the control system. If the air flow is increased while the heat dissipation in the room is constant, the temperature difference decreases.
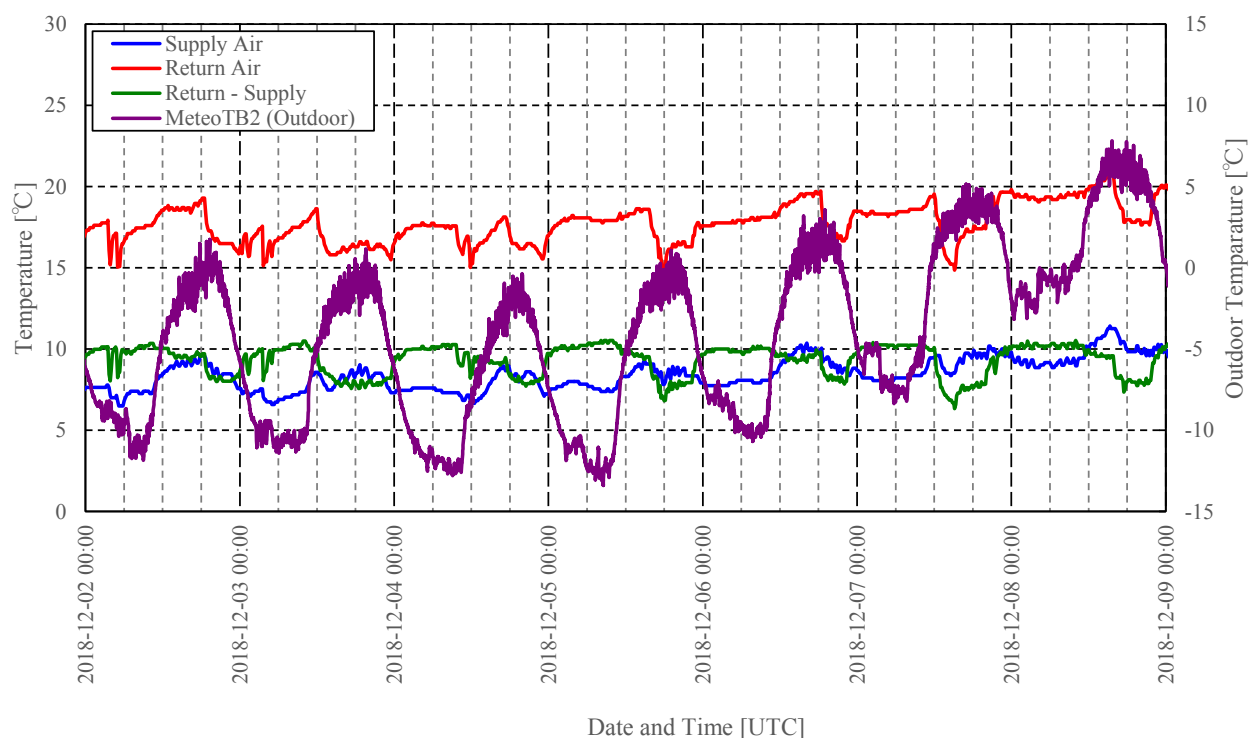
Figure 15: Close look at the supply & return air temperature, the temperature difference and the outdoor temperature (MeteoTB2) between December 2nd 2018 and December 8th 2018. Data source is the same as Figure 14 and Figure 19.
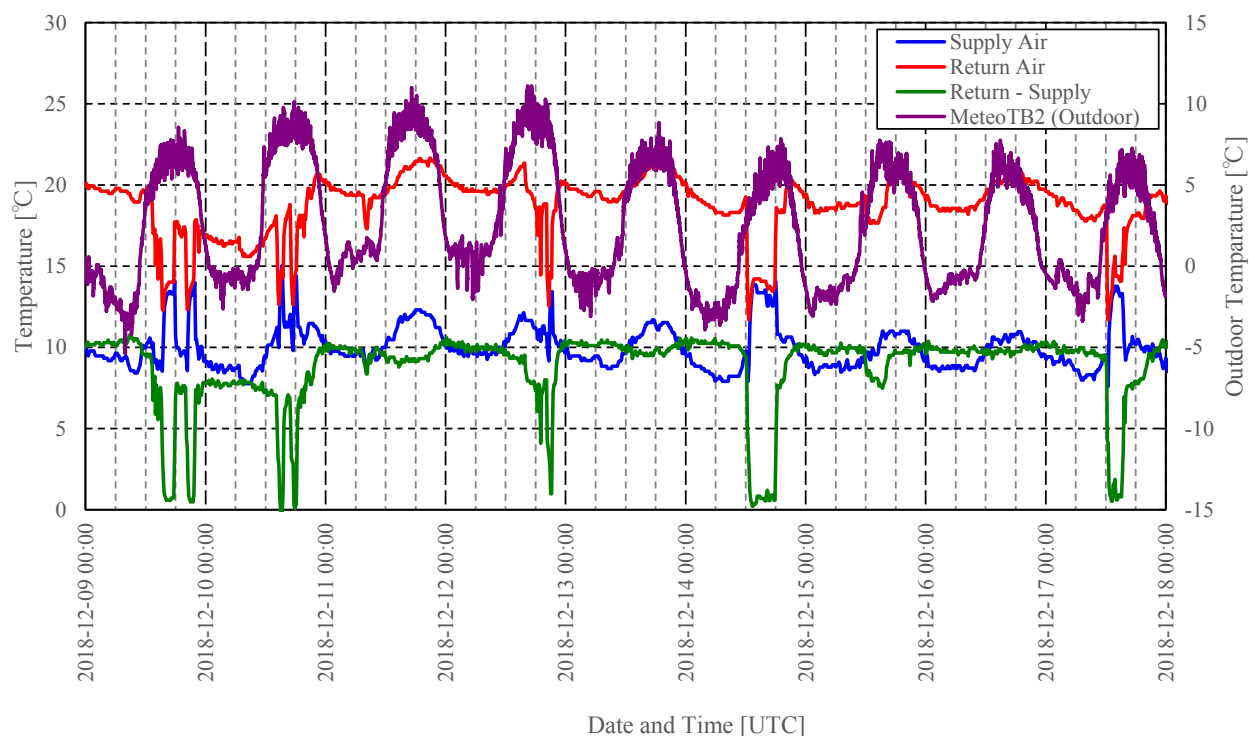
Figure 16: Close look at the supply & return air temperature, the temperature difference and the outdoor temperature (MeteoTB2) between December 9th 2018 and December 17th 2018. Data source is the same as Figure 14 and Figure 19.

3.3 Chiller

Chilled water system is well described in "AOS Tech Bldg Chilled & Hot Water Schematic" (SITE-20.01.02.05-009-A-DWG, page 29 of RD08). The water is cooled by two Air Cooled Chiller units. The chilled water is supplied to all six AHUs in the AOSTB including AHU #6. Flow rate of the chilled water to AHU #6 is adjusted by a three-way valve. From the schematic, we cannot know how this valve is controlled (maybe this valve is the same one in Figure 12), but we assume that it is controlled by Energy Management Control System based on the temperature of the supply air.
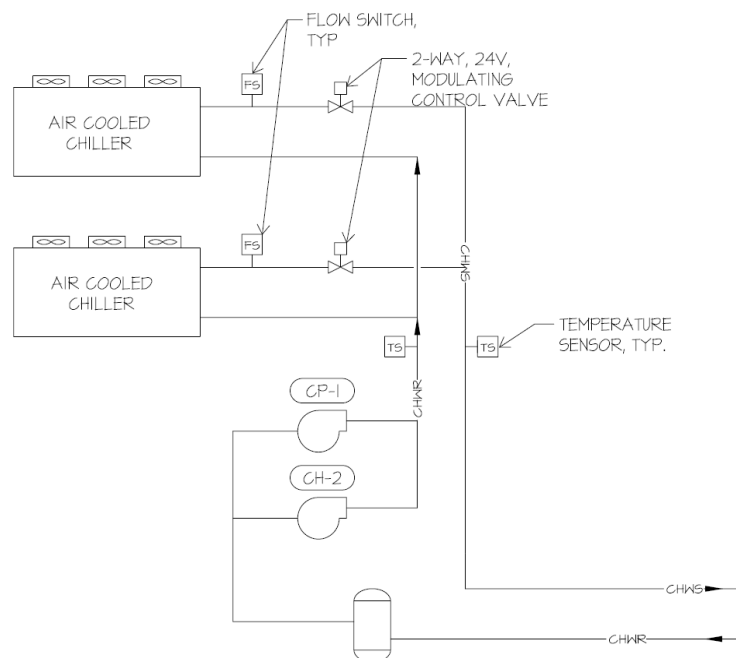
Figure 17: Excerpt from "AOS Tech Bldg Chilled & Hot Water Schematic" (SITE-20.01.02.05-009-A-DWG). Close look at the air cooled chillers.
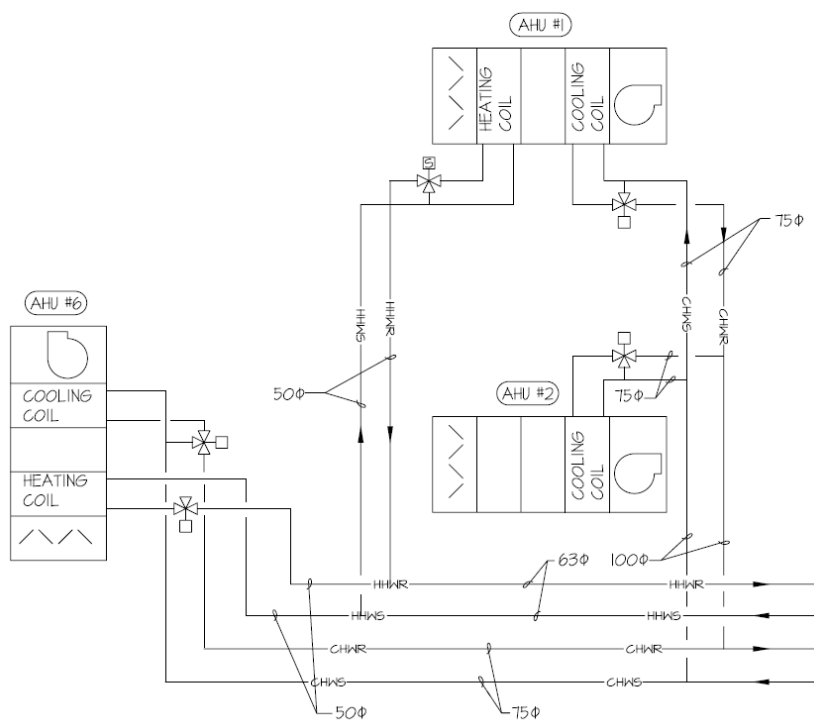
Figure 18: Excerpt from "AOS Tech Bldg Chilled & Hot Water Schematic" (SITE-20.01.02.05-009-A-DWG). Close look at the AHU #6. There is a three-way valve at the entrance of the AHU #6 in the line for CHWS.

Cooling capacity of one air cooled chiller unit is 281.2 kW according to "AOS Tech Bldg Mechanical Schedules" (SITE-20.01.02.05-011-A-DWG, page 31 of RD08) at a certain condition. Thus, the total cooling capacity of the whole AOSTB is 562.4 kW.

Table 4: Chiller Schedule, an excerpt from "AOS Tech Bldg Mechanical Schedules" (SITE-20.01.02.05-011-A-DWG)

TAG NO.		CH-1, 2
CHILLER SERVICE AND FUNCTION		WATER CHILLING
CPACITY KW		281.2
CHILLED WATER	ENTERING WATER TEMP ℃	11.1
	LEAVING WATER TEMP ℃	4.4
	GLYCOL / WATER	40%
	LPS	11.7
	ΔP M WG.	5.5
CONDENSING AIR	ENTERING ℃	23.9
	LEAVING ℃	(blank)
	LPS	(blank)
MIN CIRCUIT AMPS		211.2
ELECTRICAL SERVICE V/HZ/ϕ		400/50/3
ACCEPTABLE MANUFACTURERS		CARRIER
MODEL SHOWN		30GTN080
EER RATING		10.6
REFRIGERANT TYPE		R22
REMARKS		1.0

Note that the model of the air cooled chiller is Carrier 30GTN 080. See RD10 for more details of the chiller.

3.4 Outdoor Temperature

The performance of the air cooled chiller heavily depends on the outdoor temperature. The higher the outdoor temperature is, the lower the performance of the air cooled chiller is. Figure 19 shows the trend of the outdoor temperature measured by MeteoTB2, which is a weather station located on the roof of the AOSTB [RD11], between January 1st 2016 and December 18th 2018. The highest temperature during the period except February (annual ALMA maintenance period) was 12.3 ℃ at January 22 2016. In other two years, the highest temperature 12.1 ℃ in either January or March.
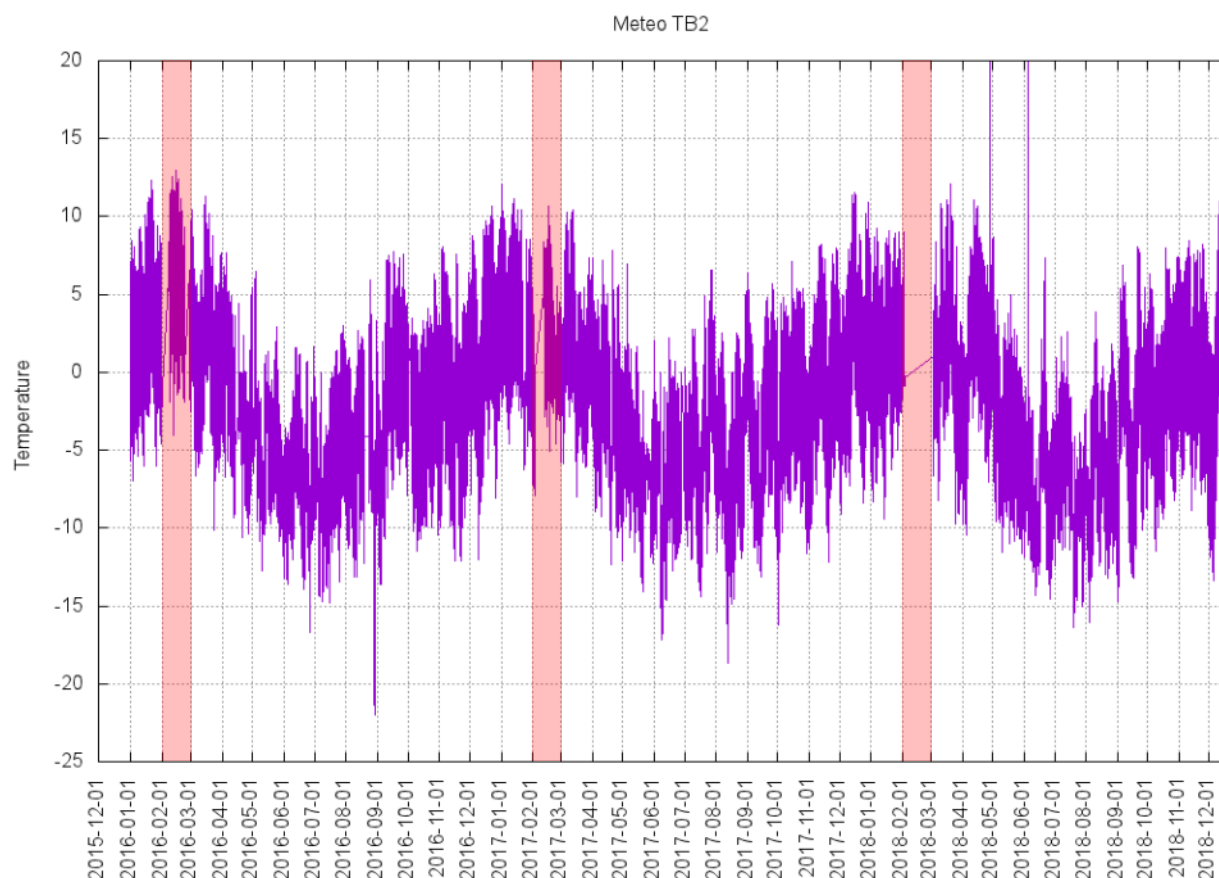
Figure 19: Trend of temperature measured by MeteoTB2. The original data were obtained from Monitor Data Service (CONTROL_WeatherStationController _MeteoTB2). The sensor reading were sampled every one minute. February perioed was hatched by red when normally ALMA is under maintenance.

Caveat: In 2018, false highest temperature 20.0 ℃ were recorded two times; (1) 2018-04-29T04:38:56.119 to 04:48:56.119 and (2) 2018-06-05T01:20:11.899 to 01:43:11.899. In these periods, the sensor reading was constant (20.0 ℃). They are considered misreported because one minute before and after the higheset temperature is recorded, the temperature was below 0 ℃ . It is very unlikely that the temperature changed by more than 20℃ within one minute.

3.5 Impact of Outdoor Temperature on ACA Correlator

Outdoor temperature has large impact on the temperature of the ACA Correlator. Figure 20 shows the trend of the outdoor temperature and U12 (TBC) temperature sensor reading in each ACA Correlator module on the hottest day in 2018 (March 20th). Within that day, the lowest outdoor temperature was around -2 ℃. while the highest was 12.1 ℃ (approximately 14 ℃ variation within one day). On the same day, the difference between the lowest and the highest temperature is 2.5 ℃ on most of the modules of the ACA Correlator. From those trends, it can be said that, roughly speaking, if the variation of the outdoor temperature is δ ℃, it causes 0.2δ ℃ temperature variation in the ACA Correlator. For example, if the outdoor temperature has 10 ℃ variation, the temperature of the ACA Correlator has approximately 2 ℃ variation.
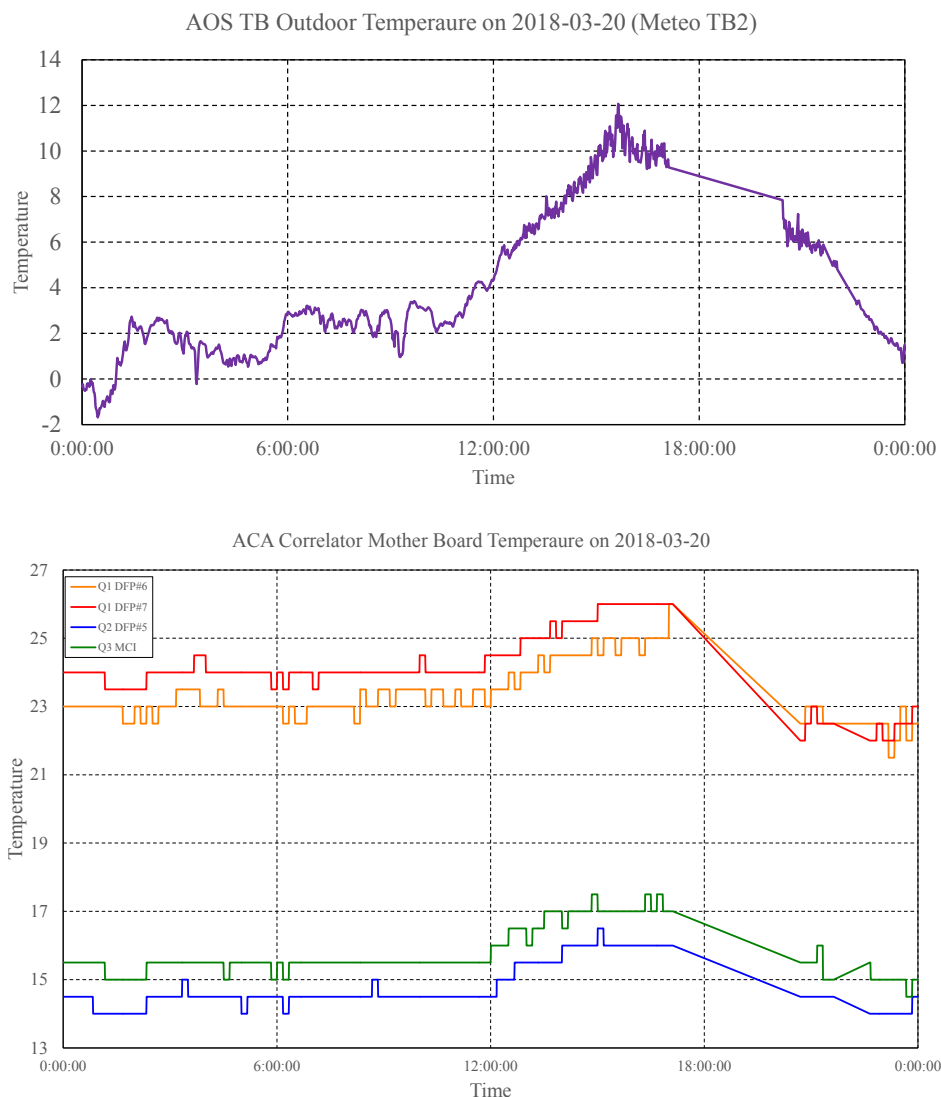
Figure 20: **Trend of outdoor temperature (upper) and the U12 (TBC) temperature sensor reading on the hottest day in 2018 (March 20th). The original data were obtained from Monitor Data Service. Among 52 modules in the ACA Corelator, the two hottest modules (Q1 DFP#6 and Q1 DFP#7) and the two coldest modules (Q2 DFP#5 and Q3 MCI) were selected to show the extremes. The temperature sensor U12 (TBC) is mounted in the mother board of each module.**

rear
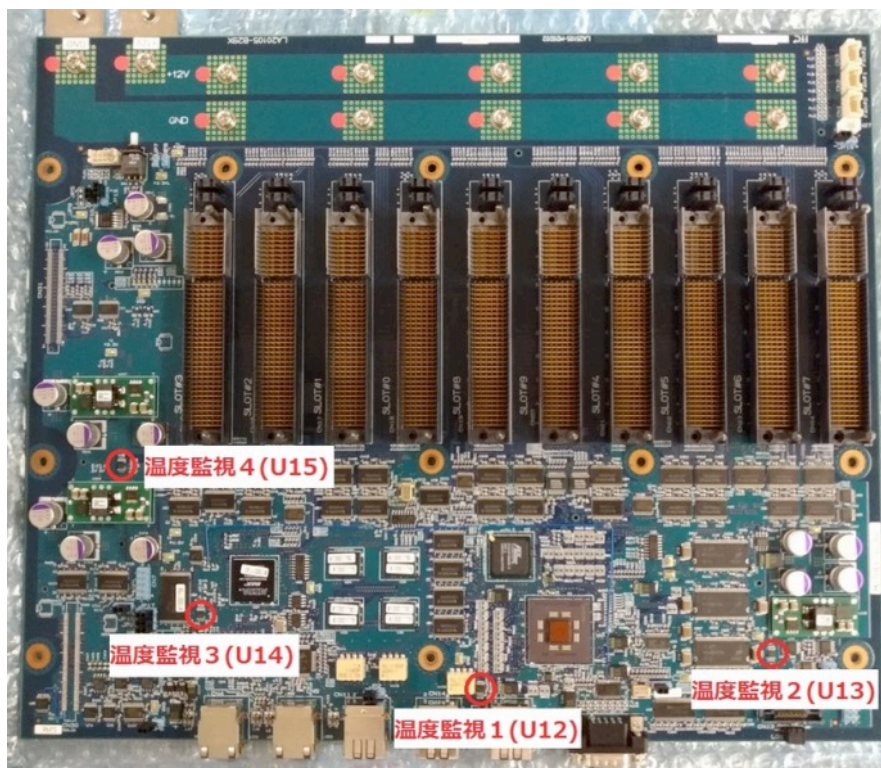
front

Figure 21: Motherboard of the ACA Correlator modules and the location of the temperature sensors. Design of the mother boards is common to all types of modules (CFP, CIP and MCI) (TBC).

Figure 22: One quadrant of the ACA Correlator, which has eight DFP modules, four CIP modules and one MCI module. There are four quadrants in total in the ACA Correlator Room.

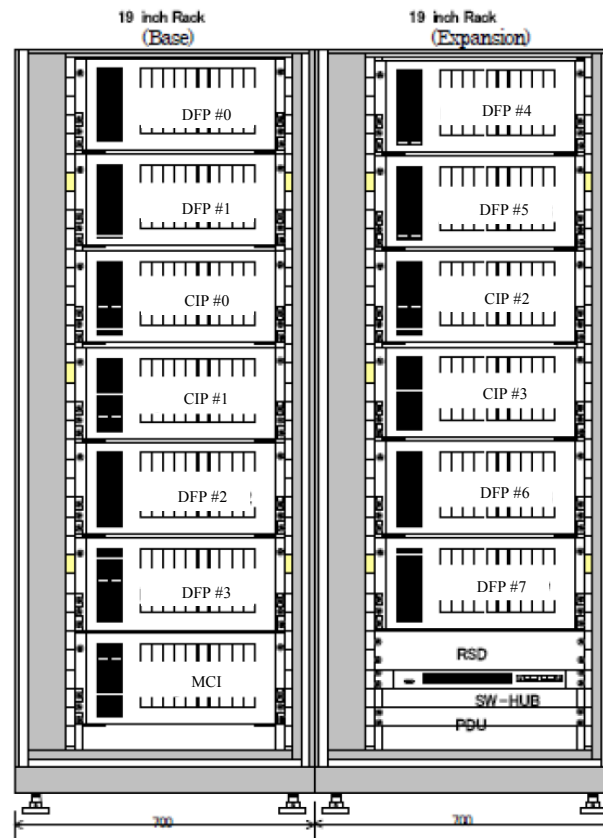## 3.6 Temperature of Inlet Air to ACA Correlator

Unfortunatly, we are not directly measuring the tempefature of the inlet air to the ACA Correlator, which is important for the following analysis. However, we can consider the maximum tempefature sensed by U12 as the maximum temperature of the inlet air. The temperature of the inlet air is thought to be the lowest among the any part of the ACA Correlator. Thus, we can say that the tempefature of the inlet air will not exceeed 26 ℃ even on the hottest day in a year (except February).

In reality, the actual temperature of the inlet air must be way below 26 ℃. It is because, although the measurement was performed in December 2018 (not the hottest month in a year), the supply air temperature of AHU #6 did not exceed 12.3 ℃ as explained in section 3.2. Thus, we believe that the maximum temperature of the inlet air to the ACA Correlator must be way below 26 ℃.

4 ACA Correlator Thermal Design

4.1 Temperature Margin of ACA Correlator

One of the most important aspects of this study is to confirm that the existing ACA Correlator will not be interrupted by the new ACA Spectrometer. The room temperature may increase due to the additional heat source (ACA Spectrometer). Thus, it is important to confirm that the temperature increase is acceptable from the view point of the ACA Correlator operation. This chapter revisits the thermal analysis of the existing ACA Correlator, which was performed in the past, to estimate how much temperature increase is acceptable.

As a result of revisiting the thermal analysis, it is concluded that up to 6.4 °C increase is acceptable.

The following sections discuss the temperature margin of the ACA Correlator from two aspects; (1) FPGA junction temperature and (2) threshold of the overheating protection.

4.1.1 FPGA Junction Temperature

The main brain of the ACA Correlator is FPGA, which consumes the power the most among the electrical components in the ACA Correlator. The manufacturer of the ACA Correlator has analyzed and measured the cooling performance of the ACA Correlator and they compiled the results in ACA Correlator Thermal Analysis Report [RD12]. According to the report, the maximum operational junction temperature of the FPGAs is 85 °C above which some performance requirement cannot be met.

Based on the measurement reported in RD12, U38(LX60) on a FFT card (slot 7) in a DFP module found to be the hottest among the other FPGAs (see section 9.7 for more details in RD12). Fujitsu measured the case temperature in a constant temperature & constant pressure chamber with three pressure settings; 760 mmHg (equivalent to ground level), 409 mmHg (equivalent to an altitude of 5,000 m, or 545 hPa) and 367.5 mmHg (equivalent to an altitude of 5,600 m). The chamber temperature was set to 28 °C.
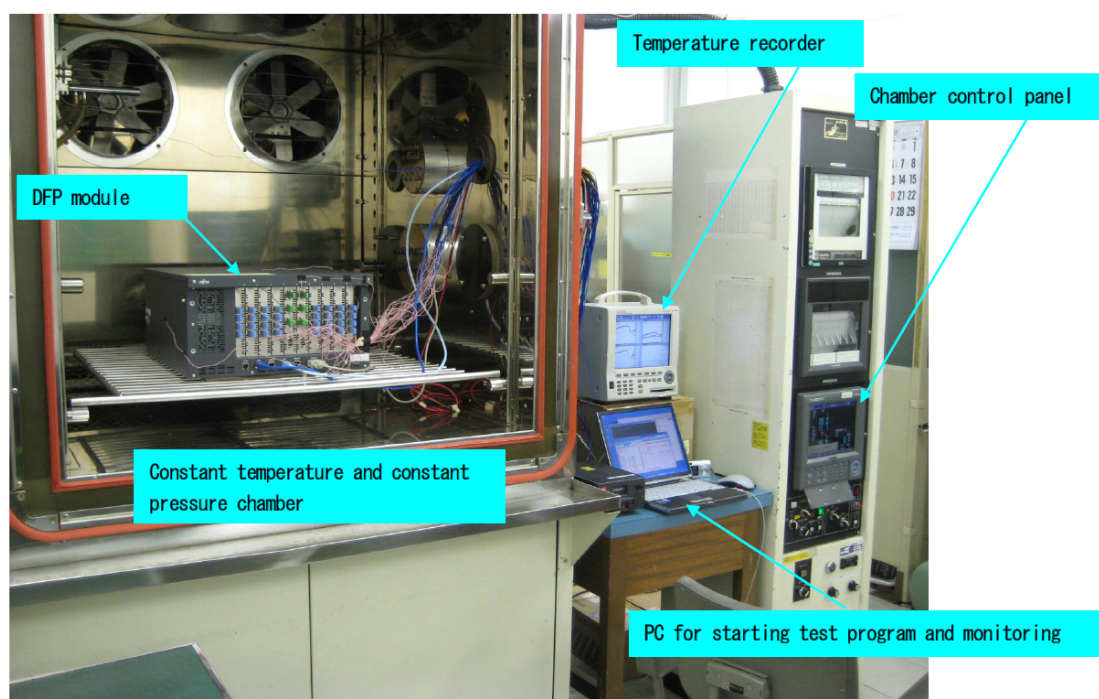
Figure 23: Temperature measurement set-up of a DFP module in a constant temperature/pressure chamber [RD12].

As a result of the measurement at the pressure of 409 mmHg (5,000 m), the case temperature of U38(LX60) reached 73.8 °C. The temperature of the inlet air was also measured at the same time, which was actually 30.1 °C. The power consumption of this FPGA is 9.5 W and the thermal resistance between the case surfaces to the junction is 0.2 °C/W. So, the junction temperature is estimated to be $73.8 + 9.5 \times 0.6 = 79.5$ °C at the time of the measurement.
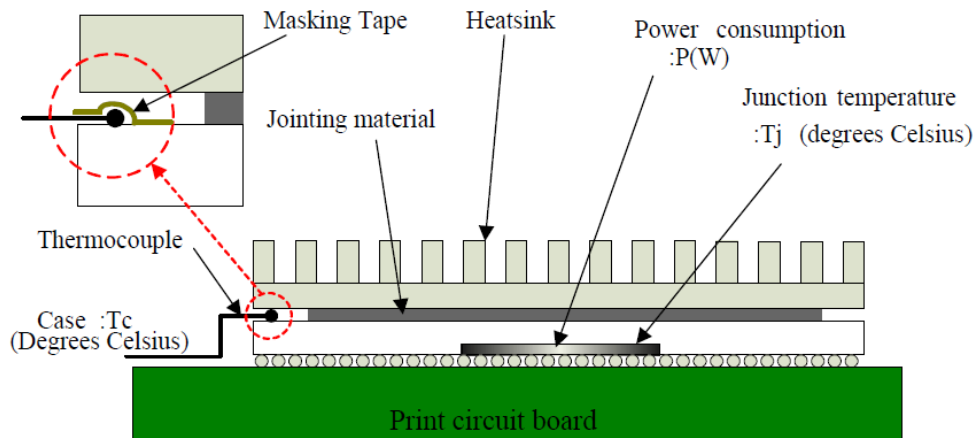
Figure 24: The location of the thermocouple when the temperature measurement was made [RD12].

If the temperature of the inlet air is 26 ℃, the junction temperature will be 79.5 – 30.1 + 26 = 75.4 ℃. As already discussed in section 3.6, the inlet air temperature will not exceed 26 ℃ in the current situation before installing the new ACA Spectrometer. Because the maximum operational junction temperature of the FPGAs is 85 ℃, the hottest FPGA still has 85 – 75.4 = 9.6 ℃ margin or more. In other words, if the inlet air temperature (or room temperature) was increased by 9.6 ℃ due to the heat dissipation of the new ACA Spectrometer, the junction temperature would not exceed 85 ℃.

Note that a margin in design typically takes into account measurement errors and variance of individuals. Actually, in RD12, Fujitsu quoted the measurement result at 367.5 mmHg (5,600 m) to evaluate the margin. The measurement result at 367.5 mmHg was 3.2 ℃ higher than the one at 409 mmHg (5,000 m). Thus, 3.2 out of 9.6 ℃ should be reserved, and we can conclude that the temperature increase caused by the new ACA Spectrometer is acceptable up to 6.4 ℃.

4.1.2 Overheating Protection

Another aspect of the ACA Correlator thermal design is overheating protection. Each board in the ACA Correlator modules has one or more temperature sensors to detect overheating. Once one of the temperature sensor reading goes over a certain threshold, it interrupts the ACA Correlator and notifies the ACA Correlator computers of the event with the failure code of 0x5901 according to RD13.

Category1 (4bit, HEX)	Category2 (4bit, HEX)		Category3 (8bit, HEX)		Description
2	8	Software interruption	00	Signal detection	Caught an exception with the signal ID. The module is turned off power.
5	9	Hardware interruption	00	Voltage, temperature or fan speed of the mother board	The motherboard detected out of specified voltage, the temperature, or the fan speed. The module is turned off power.
			01	Voltage, temperature, or fan speed of the board	A board detected out of specified voltage, the temperature, or the fan speed. The module is turned off power.
1			02	Unspecified interruption	Other than those above.
4	A	Software detected hardware execution error	00	Register verification failure	Failed to verify of the register, or detected a read check error of SDRAM after writing.
			01	Device busy	The FPGA on the board is busy so that the process stops.
			02	Time out	The hardware control command timed out. E.g., time out to reconfigure the FPGA, time out to read/write the SDRAM.
1			03	Buffer underrun error (Delay correction)	No data on the delay correction register of the DFP module. Probably, "Set delay compensation data" command is not received in time.

Figure 25: Failure code common to all ACA Correlator modules [RD13]. The failure code for overheating is emphasized with a red rectangle. In a strict sense, the failure code of 0x5901 also includes overvoltage and fan failures.

Fortunately or unfortunately, this failure was triggered by LM75#4 of Q0 DFP#6 FFT#3 on June 25th 2018 16:46:57 (the failure event can be found with a Kibana query: `Host:"coj-cc-1" AND`

`Process:"CMD_TRANSFER" AND text:"failureCode[5901]:"`). At that time, all quadrants experienced very high temperature in around 16:40, which is thought to be a trouble of the HVAC system. The temperature readings of all temperature sensors are not archived in Monitor Data Service, but the temperature trend of the temperature sensor U12 (TBC) was recorded as shown in Figure 26.
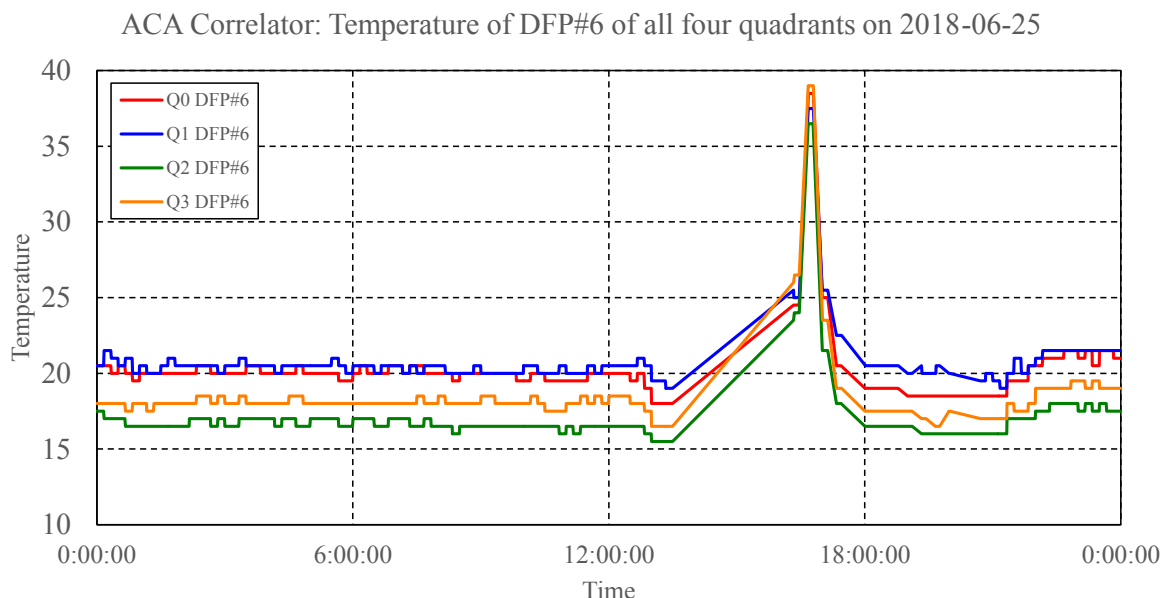
Figure 26: Temperature trend of DFP module #6 in all four quadrants on the day of the overheating event.

When the overheating failure happened, the temperature reading of Q0 DFP #6 was 38.5 ℃. Typically, the temperature reading of that module is around 20 ℃ and it reaches the highest temperature 24 ℃ in summer. So, it is inferred that there is 38.5 – 24 = 14.5 ℃ margin until the overheating protection is activated.

4.2 Air Flow

Fujitsu finally selected Sanyo Denki 9GL1212J101 as the fan for the ACA Correlator modules [RD12]. Table 5 shows the specification of this fan.

Table 5: Specification of the fans for the ACA Correlator (Sanyo Denki 9GL1212J101) [RD12].

Maximum Airflow	5.1 m³/min
Rated Electric Current	1.9 A
Rated Fan Speed	4800 RPM
Rated Voltage	DC12V
Lifetime	60000 hours

This fan rotates at a maxium of 4800 RPM and is capable of generating an air flow of 5.1 m³/min at most at the ground level.

At AOS, the fan speed is a bit faster than 4800 RPM. Table 6 shows average fan speed on December 16th 2018 of every ACA Correlator module. Average rotation speed of all fans is 5368 RPM, which is 12 % faster than the specification, which is consistent with the fan speed measurement of a prototype ASM (see subection 2.1.6). It is thought to be an effect of low pressure at high site.

Table 6: Average fan speed on 16th December 2018 (UTC) of all ACA Correlator modules. Unit is RPM. Data source is Monitor Data Service.

		Q0	Q1	Q2	Q3
CIP0	fan#0	5408	5430	5403	5190
	fan#1	5309	5185	5213	5092
	fan#2	5305	5311	5324	5078
CIP1	fan#0	5485	5459	5543	5249
	fan#1	5326	5149	5218	5131
	fan#2	5183	5144	5252	5120
CIP2	fan#0	5551	5402	5441	5456
	fan#1	5347	5269	5218	5292
	fan#2	5331	5213	5254	5300
CIP3	fan#0	5689	5495	5429	5562
	fan#1	5381	5268	5068	5314
	fan#2	5340	5274	5230	5292
DFP0	fan#0	5608	5249	5498	5356
	fan#1	5391	5418	5351	5127
	fan#2	5171	5565	5300	5128
DFP1	fan#0	5408	5511	5614	5321
	fan#1	5261	5230	5435	5132
	fan#2	5296	5408	5508	5104
DFP2	fan#0	5580	5559	5625	5357
	fan#1	5271	5329	5349	5144
	fan#2	5232	5379	5443	5096
DFP3	fan#0	5403	5527	5577	5365
	fan#1	5203	5314	5413	5132

	fan#2	5220	5404	5340	5190
DFP4	fan#0	5510	5540	5637	5530
	fan#1	5360	5347	5392	5268
	fan#2	5266	5239	5237	5314
DFP5	fan#0	5518	5585	5517	5467
	fan#1	5225	5355	5357	5229
	fan#2	5325	5405	5557	5445
DFP6	fan#0	5623	5414	5547	5580
	fan#1	5465	5312	5325	5335
	fan#2	5398	5274	5467	5371
DFP7	fan#0	5564	5576	5556	5551
	fan#1	5492	5440	5442	5465
	fan#2	5495	5442	5381	5267
MCI	fan#0	5402	5399	5380	5479
	fan#1	5400	5324	5323	5537
	fan#2	5605	5379	5351	5608

Therefore, the maximum air flow of one fan can be 5.1 × 1.12 = 5.7 m³/min. Because there are three fans in each module, the maximum air flow of one module is 17.1 m³/min, and the total maximum air flow of the whole ACA Correlator is 17.1 × 52 = 891 m³/min. The actual air flow must be less than that value due to the system impedance (= flow resistance) of the module.

5 Impact of ACA Spectrometer

Combining the thermal design of the ACA Spectrometer, the current status of the ACA Correlator Room and AHU #6 and the ACA Correlator thermal design, this chapter discusses the impact of the new ACA Spectrometer on the whole AOSTB, return temperature of AHU #6 and the average temperature of the exhaust air from both the ACA Correlator and the ACA Spectrometer.

5.1 Impact to the Whole AOSTB

The heat dissipation from the new ACA Spectrometer is estimated to be 7.7 kW as explained in chapter 2 while the cooing capacity of the air cooled chiller for the whole AOSTB is 562.4 kW in total as explained in section 3.3 at a certain condition (see Table 4 for more details). The heat dissipation of the ACA Spectrometer is only 1.4 % of the total cooing capacity.

This chapter evaluates impact to the whole AOSTB using a very simplified thermal model. Let's assume that the average inside temperature of the AOSTB is 25 °C while the outdoor temperature is 12.3 °C which is the highest temperature during the science operation as explained in section 3.4. Plus, let's also assume that the total heat dissipation from the AOSTB to the outdoor is the same as the cooling capacity, 562.5 kW. The heat from the inside comes out to the outdoor through the chilled water system and the walls. Here we use a very simplified thermal model: we consider that there is only one thermal resistance between the inside and the outdoor as shown in Figure 27. This thermal resistance includes the cooling performance of the chilled water system and the thermal insulation performance of the walls. Now let's assume that this thermal resistance is constant: (25.0 – 12.3) / 562.4 = 0.0226 °C/kW.
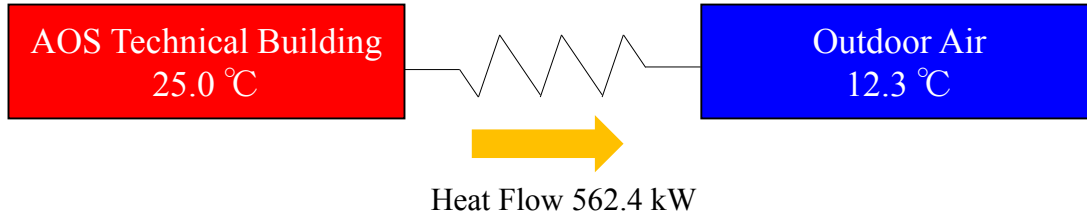
Figure 27: Simplified thermal model of the AOSTB and the outdoor air.

Once we add an additional heat source (ACA Spectrometer) of 7.7 kW, the heat flow increased to 569.9 kW and the inside temperature of the AOSTB increases to 0.0226 × 569.9 + 12.3 = 25.2 °C.
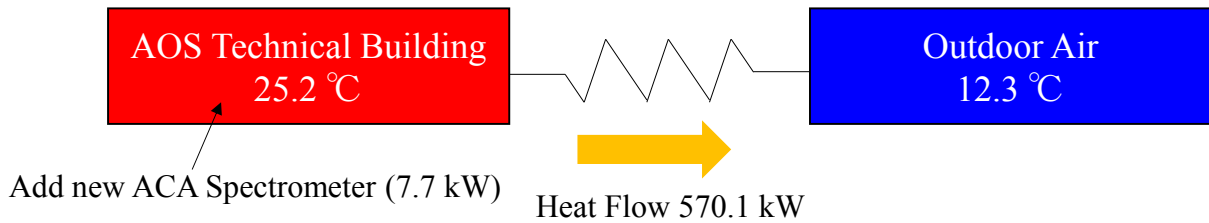
Figure 28: Simplified thermal model of the AOSTB with the new ACA Spectrometer and the outdoor air.

The analysis using the simplified thermal model indicates that the new ACA Spectrometer may increase the average inside temperature of the AOSTB by 0.2 °C. In reality, the temperature of the ACA Correlator Room will increase the most while the other rooms should experience smaller temperature increase. In addition, the chiller should have performance margin. So, the author believes that the temperature increase to the other rooms in the AOSTB is around 0.1 °C or less, which is less than the variance caused by the change of the outdoor temperature. So, the impact of the new heat source to the whole AOSTB is negligible.

Note that the biggest uncertainty in this simplified model is the heat dissipation from the AOSTB. The author believes that, it is normally less than the total cooling capacity of the chillers, so it is assumed so in this report. Maybe it can be confirmed from the total power consumption during the science operation assuming that almost all power were finally converted to heat.

In either case, the estimated temperature increase 0.2 °C caused by the new ACA Spectrometer is way below the acceptable temperature margin 6.4 °C of the ACA Correlator (see section 4.1 for more details of how the temperature margin was yielded).

5.2 Return Temperature of AHU #6 (ACA Correlator Room)

In this section, the return temperature of AHU #6 will be estimated given that both the ACA Correlator and the new ACA Spectrometer are in full operation.

First of all, air flow of AHU #6 is estimated here because we do not know the actual air flow while the maximum is 680 m^3/min. Without the ACA Spectrometer, the air flow can be calculated as

$$Q_{AHU\#6} = \frac{q_{CORR}}{\rho C_p \Delta T_{AHU\#6}} \tag{3}$$

where q_{CORR} is the total heat dissipation in the ACA Correlator Room in watt, ρ is the air density in kg/m^3, C_p is specific heat of the air (see Appendix A for more details) and $\Delta T_{\text{AHU\#6}}$ is the temperature difference between supply and return air of AHU #6 in °C. Figure 14 shows that, except periods when the ACA Correlator is obviously suspended, the temperature difference is between 7 and 11 °C. So, possible range of the air flow can be written as below

$$\frac{q_{\text{CORR}}}{\rho C_p \times 11} < Q_{\text{AHU\#6}} < \frac{q_{\text{CORR}}}{\rho C_p \times 7} \tag{4}$$

$$0.14 \times 10^3 \times q_{\text{CORR}} < Q_{\text{AHU\#6}} < 0.22 \times 10^3 \times q_{\text{CORR}} \tag{5}$$

The only uncertainty is the actual heat dissipation in the ACA Correlator Room. We already know the maximum heat dissipation in the room is 77 kW (see section 3.1), so let's try to substitute q_{CORR} with 77×10^3 W, which yields

$$10.7 \, \text{m}^3/\text{sec} < Q_{\text{AHU\#6}} < 16.8 \, \text{m}^3/\text{sec} \tag{6}$$

or

$$640 \, \text{m}^3/\text{sec} < Q_{\text{AHU\#6}} < 1005 \, \text{m}^3/\text{min} \tag{7}$$

Apparently, this is not true because the maximum air flow of AHU #6 is 680 m^3/min. If the heat dissipation in the room was 77 kW all the time, the actual heat dissipation would almost always exceed the maximum air flow. So, the actual heat dissipation is smaller than 77 kW, at least, when the temperature difference is smaller than 10.3 °C.

To simply the problem, let's ignore the case where the ACA Correlator is not in full operation. As already discussed in section 3.2, the temperature difference is typically approximately 10 °C when the ACA Correlator including the associated computers are thought to be in full operation. At that time, the air flow of AHU #6 can be written as

$$Q_{\text{AHU\#6}} = \frac{q_{\text{CORR}}}{\rho C_p \times 10} = 0.15 \times q_{\text{CORR}} \tag{8}$$

Table 7 shows $Q_{\text{AHU\#6}}$ for various q_{CORR}.

Table 7: Relation between q_{CORR} and $Q_{\text{AHU\#6}}$ when the temperature difference ΔT is 10 °C.

q_{CORR}	q_{CORR} / 77 kW	$Q_{\text{AHU\#6}}$
77.0 kW	100 %	704
73.1 kW	95 %	669
69.3 kW	90 %	633
65.5 kW	85 %	598
61.6 kW	80 %	563

The author believes that the estimation of the heat dissipation (65 kW) of the ACA Correlator is almost true because it is the main heat source, and heard that there was a history to try to reduce the power consumption during the design. Actually, according to one measurement [RD18], the actual

power consumption of one quadrant was 15.8 kW, which means 63 kW in total excluding the ACA Correlator computers. In contrast, it seems that the heat dissipation estimation of the associated computers (12 kW) may include large margin in the same way as the heat dissipation estimation of the ASMs. So, let's assume here that the heat dissipation is larger than 65 kW. Then, the lower boundary of the air flow can be obtained as

$$\frac{65 \times 10^3}{\rho C_p \times 10} < Q_{\text{AHU\#6}} \tag{9}$$

$$594 \text{ m}^3/\text{min} < Q_{\text{AHU\#6}} \tag{10}$$

The upper boundary of the heat dissipation of the ACA Correlator and the associated computers can be derived from the maximum air flow of $Q_{\text{AHU\#6}} = 680$ m³/min

$$q_{\text{CORR}} < \rho C_p \times 10 \times 680 \div 60 \tag{11}$$

$$q_{\text{CORR}} < 74 \text{ kW} \tag{12}$$

Now that we have estimated the air flow of AHU #6 ($Q_{\text{AHU\#6}}$) and the heat dissipation of the existing equipment (q_{CORR}), let's estimate how high the temperature difference ΔT will be when the new ACA Spectrometer is installed. The equation is

$$\Delta T = \frac{q_{\text{CORR}} + q_{\text{SP}}}{\rho C_p Q_{\text{AHU\#6}}} \tag{13}$$

As already discussed, the heat dissipation of the new ACA Spectrometer is below 7.7 kW, hence,

$$q_{\text{SP}} < 7.7 \text{ kW} \tag{14}$$

Thus, the upper boundary of ΔT can be obtained as

$$\Delta T < \frac{(74 + 7.7) \times 10^3}{\rho C_p \times 594 \div 60} = 12.5 \text{ °C} \tag{15}$$

This is 2.5 °C higher than before installing the ACA Spectrometer. As already discussed in 5.1, the heat dissipation from the ACA Spectrometer is only 1.4 % of the cooing capacity of the AOSTB. Thus, it is likely that the supply air temperature of AHU #6 will stay the same even after installing the ACA Spectrometer, which means that the new ACA Spectrometer will simply increase the return air temperature by 2.5 °C at most.

5.3 Average Outlet Temperature from ACA Correlator and ACA Spectrometer

Temperature of the exhaust air from the ACA Correlator and the ACA Spectrometer matters because the workers may stand behind them. To simplify the problem, in this section, the average temperature of the exhaust air from both the ACA Correlator and the ACA Spectrometer (= average temperature of the hot aisles) will be estimated. Assuming that the inlet air temperature is the same for both ACA Correlator and the ACA Spectrometer, the average temperature of the exhaust air can be written as

$$\Delta T_{\text{ACA}} = \frac{Q_{\text{CORR}} \Delta T_{\text{CORR}} + Q_{\text{SP}} \Delta T_{\text{SP}}}{Q_{\text{CORR}} + Q_{\text{SP}}} \tag{16}$$

where

- Q_{CORR} Total Air Flow of the ACA Correlator
- Q_{SP} Total Air Flow of the ACA Spectrometer
- ΔT_{CORR} Temperature Difference between Inlet and Exhaust Air Temperature of the ACA Correlator
- ΔT_{SP} Temperature Difference between Inlet and Exhaust Air Temperature of the ACA Spectrometer

Q_{CORR} and ΔT_{CORR} stays the same regardless whether the ACA Spectrometer is newly installed or not. Now we are interested in how high the average temperature ΔT_{ACA} will be after the ACA Spectrometer is installed. Currently, before installing the ACA Spectrometer, the average temperature of the exhaust air is ΔT_{CORR}. Thus, the temperature increase caused by the new ACA Spectrometer is

$$\Delta T'_{ACA} = \Delta T_{ACA} - \Delta T_{CORR} \tag{17}$$

Unfortunately, we have never measured ΔT_{CORR} or ΔT_{SP}, but we can estimate them from the heat dissipation of the ACA Correlator q_{CORR} and q_{SP}.

$$\Delta T_{CORR} = \frac{q_{CORR}}{\rho C_p Q_{CORR}} \tag{18}$$

$$\Delta T_{SP} = \frac{q_{SP}}{\rho C_p Q_{SP}} \tag{19}$$

With these relations, $\Delta T'_{ACA}$ can be expanded to

$$\Delta T'_{ACA} = \frac{q_{SP} Q_{CORR} - q_{CORR} Q_{SP}}{\rho C_p Q_{CORR}(Q_{CORR} + Q_{SP})} \tag{20}$$

Partial derivatives of $\Delta T'_{ACA}$ with respect to q_{SP}, q_{CORR}, Q_{SP} and Q_{CORR} are

$$\frac{\partial(\Delta T'_{ACA})}{\partial q_{SP}} = \frac{1}{\rho C_p(Q_{CORR} + Q_{SP})} \tag{21}$$

$$\frac{\partial(\Delta T'_{ACA})}{\partial q_{CORR}} = -\frac{Q_{SP}}{\rho C_p Q_{CORR}(Q_{CORR} + Q_{SP})} \tag{22}$$

$$\frac{\partial(\Delta T'_{ACA})}{\partial Q_{SP}} = -\frac{q_{CORR} + q_{SP}}{\rho C_p(Q_{CORR} + Q_{SP})^2} \tag{23}$$

$$\frac{\partial(\Delta T'_{ACA})}{\partial Q_{CORR}} = \frac{q_{CORR} Q_{SP}}{\rho C_p Q_{CORR}{}^2(Q_{CORR} + Q_{SP})} \tag{24}$$

Because all the variables and constants in the above equations are positive,

$$\frac{\partial(\Delta T'_{ACA})}{\partial q_{SP}} > 0 \tag{25}$$

$$\frac{\partial(\Delta T'_{ACA})}{\partial q_{CORR}} < 0 \tag{26}$$

$$\frac{\partial(\Delta T'_{\text{ACA}})}{\partial Q_{\text{SP}}} < 0 \tag{27}$$

$$\frac{\partial(\Delta T'_{\text{ACA}})}{\partial Q_{\text{CORR}}} > 0 \tag{28}$$

The above expressions of inequality indicate that $\Delta T'_{\text{ACA}}$ takes a maximum value when q_{SP} and Q_{CORR} are maximum, and when q_{CORR} and Q_{SP} are minimum.

- Maximum of q_{SP}: 7.7 kW (see chapter 2)
- Maximum of Q_{CORR}: 891 m³/min (see section 4.2)
- Minimum of q_{CORR}: 65 kW (see section 5.2)
- Minimum of Q_{SP}:   4.1 × 4 = 16.4 m³/min (see subsection 2.1.6)

When we substitute q_{SP}, Q_{CORR}, q_{CORR} and Q_{SP} with the above values, we get

$$\Delta T'_{\text{ACA}} < 0.66 \tag{29}$$

So, the average temperature of the exhaust air from both the ACA Correlator and the ACA Spectrometer can be increased by up to 0.66 ℃ when the new ACA Spectrometer is installed. This is negligible amount. Furthermore, because the estimation of the minimum Q_{SP} is very underestimated to be on the safe side, the actual temperature increase will be much less than 0.66 ℃.

6 Summary

This study investigated impacts of the new ACA Spectrometer on the existing HVAC system, the ACA Correlator operation and the room temperature. Below is the summary of the study.

- Additional 7.7 kW heat dissipation from the new ACA Spectrometer is only 1.4 % of the total cooling capacity of the AOSTB chilled water system. It may increase room temperature by up to 0.2 ℃, which is way below the temperature margin of the ACA Correlator (6.4 ℃).
- Return air temperature of AHU #6 will be increased by up to 2.5 ℃ after installing the ACA Spectrometer.
- The average temperature of the exhaust air from both the ACA Correlator and the ACA Spectrometer will be increased by up to 0.66 ℃ after installing the ACA Spectrometer.

Though this study, the author believes that additional heat dissipation generated by the new ACA Spectrometer is acceptable. However, this study made several assumptions to develop quantitative arguments. The author believes that these assumptions are reasonable, but the estimation is yet to be verified during AIV.

1. Measure the total power consumption of the existing ACA Correlator and the associated computers. The power consumption of the computers, network switches and other devices connected to PDUs can be measured by reading the current sensor in the PDUs. For the measurement of the power consumption of the ACA Correlators, a portable current transformer and voltage meter may be needed.
2. Measure total power consumption of the new ACA Spectrometer when software implementation is completed and verify that it is below 7.7 kW.
3. In December, after installing the ACA Spectrometer, put both the ACA Correlator and the ACA Spectrometer in full operation and measure the supply air temperature and the return air temperature of the AHU #6. Verify that the supply air temperature stays the same as the

measurement result in December 2018 taking into account the outdoor temperature, and that the return air temperature does not increase by more than 2.5 ℃.

4. In December, put only the ACA Correlator in full operation and measure the average temperature in the hot aisles. Then, put the ACA Spectrometer in full operation additionally and measure the same temperature again and verify that the temperature increase is less than 0.66 ℃.

The verification results are important to confirm that the estimation in this study is correct and there is no unexpected impact to the ACA Correlator, the ACA Correlator Room and the AOSTB. They will be also one of the important inputs to future extension of the ACA Spectrometer. For example, once a new feature is requested to the ACA Spectrometer, the power consumption of the ASMs would increase and we will be able to know how much the power consumption increase is acceptable from the view point of cooling. Or, if the existing ACA Correlator will be replaced by a new one (e.g. a GPU-based Correlator), the performance of the existing HVAC will be one of various constraints on the design.

Appendix A   Air Density and Specific Heat in AOSTB

According to ENVI-0070-0/R in RD14,

All ALMA equipment shall be compatible with an ambient air pressure of 550 mbar ± 60 mbar, which corresponds to an air density of 0.7214 kg/m3 (typical average).

It is not clear at which temperature the air density was evaluated. It can be thought to be very low (at least, below 0 ℃) because this is the environmental requirement for the equipment outdoor the building. RD12 quoted this air density for the thermal analysis, but the author thinks it overestimates the cooling performance because the temperature in the building is higher than outdoor and the higher the temperature is, the lower the air density is.

Therefore, air density is derived in the following manner for this study. Molar gas constant R is 8.3 J/(mol•K) according to [NIST Reference on Constants, Units and Uncertainty](). Molar mass of dry air M is 2.9×10^{-2} kg/mol. Thus, the air density ρ [kg/m^3] can be derived as

$$\rho = \frac{MP}{RT} \qquad (30)$$

where P [Pa] is pressure and T [K] is temperature. At 409 mmHg (545 Pa, equivalent to barometric pressure at the altitude of 5,000 m) and 20 ℃ (representative temperature in the ACA Correlator room), the air density is 0.65 kg/m^3. This study quotes this number in all placed for consistency instead of 0.7214 kg/m^3.

Specific heat of air C_p does not depend a lot on pressure or temperature. This study consistently assumes that it is 1.01×10^3 J/(kg•℃) at 20 ℃.

Appendix B   Power Consumption of ASM Chassis Fan

The model of the ASM chassis fan is Delta PFR0912XHE-A01 (or FAN-0151L4 in Supermicro eStore). The specification of this fan can be found in RD03 and the major specifications are copied in Table 8. Unfortunately, RD03 does not have information about the power consumption. So, the specification of a similar model PFR0912XHE-SP00 is also copied in Table 8.

Table 8: Specification of chassis fans (PFR0912XHE-A01 and PFR0912XHE-SP00).

	PFR0912XHE-A01 [RD03]	PFR0912XHE-SP00 [RD04]
Dimensions	92L x 92H x 38W [mm]	92L x 92H x 38W [mm]
Fan Speed	11500 RPM	11500 RPM ± 10%
Acoustic Noise Level	69.6 dBA	71 (max. 75.5) dBA
Maximum Airflow Rate	185.7 CFM	185.55 (min. 166.98) CFM
Input Current	3.6 A	3.70 (max. 4.50) A
Input Power	(not specified)	44.40 (max. 54.0) W
Maximum Air Pressure		64.10 (min. 51.92) mmH$_2$O
Rated Voltage		12 VDC
Operation Voltage		7.0 – 13.2 VDC

In this study, the specification in RD03 is quoted except the power consumption. The maximum power consumption of the chassis fan is assumed to be the same as PFR0912XHE-SP00, 54.0 W, in this study.

Appendix C   Air Flow and Static Pressure

Normally, air flow in a fan specification is "maximum" air flow when there is no resistance. Typically, fans are attached to an enclosure or a room and it has some objects to be cooled, which unfortunately blocks a smooth air flow. Such resistance drops air pressure, hence the air flow drops. A P-Q curve in a fan specification describes that behavior, for example, as can be seen in Figure 29. P is static pressure that the fan can generate and Q is air flow. The P-Q curve tells us that when there is no resistance (no pressure drop), the air flow is maximum (185.55 CFM), and that it cannot transport air when the pressure drop is higher than 64.10 mmH$_2$O.
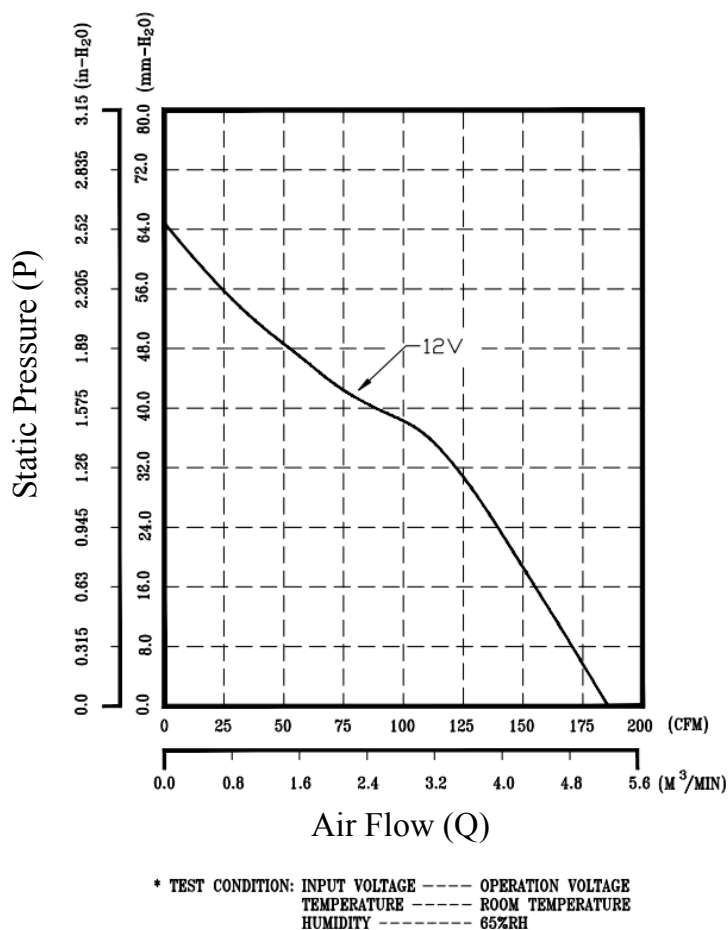
Figure 29: P-Q curve of PFR0912XHE-SP00 [RD04]. Axis titles were added by the author.

Given a certain P-Q curve, actual air flow is determined by flow resistance in the enclosure or the room to which the fan is attached to. The flow resistance is usually described as "system impedance curve" in the same chart as shown in Figure 30. According to RD15,

When air is introduced into a system, it will encounter resistance due to the layout of the system. It is the pressure drop that causes the resistance. The pressure drop (or, the resistance) goes higher when more flow is trying to pass through the system. As a result, we may envision that there is another P-Q like curve, which is commonly called the system characteristic curve. The curve tells the relation between the system impedance and flow rate. A widely used empirical relation between the two is

$$\Delta P = kQ^n \tag{31}$$

Where ΔP is the system impedance, Q is the flow rate and K is the system's characteristic constant and n is the flow factor with value between 1 and 2. For laminar flow n = 1. For turbulent flow, n = 2.

The larger the resistance is, the larger *k* is. For example, in Figure 30, the curve A represents a system impedance curve of which a system that has relatively large resistance while the curve C represents a system impedance curve of which a system has relatively small resistance. The actual air flow is determined by the cross section between a P-Q curve and a system impedance curve. For

example, if a P-Q curve and a system impedance curve A is given as show in Figure 30, air flow of that system becomes Q_A.
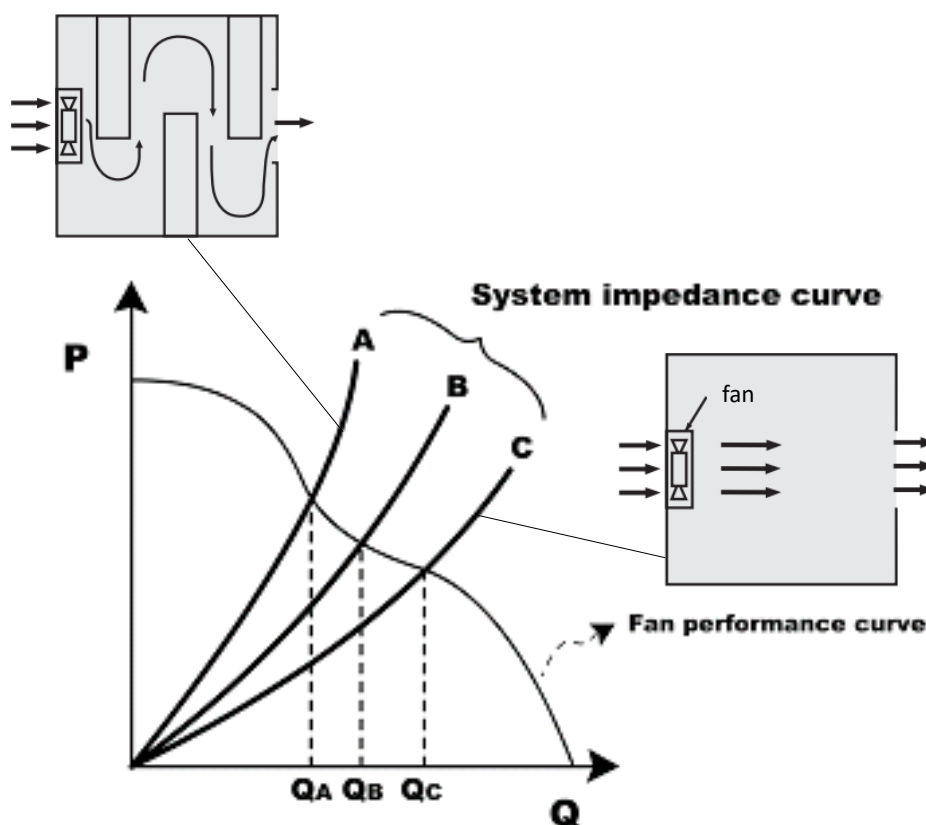

Figure 30: An example P-Q curve of a fan and an example system impedance curve in the same chart. [RD15]

Now the question is what if we have two or more fans? There are two types of operation of multiple fans. One is parallel and the other is series.

In parallel operation, multiple fans are set up side by side. In this configuration, the maximum air flow is multiplied by the number of the fans. It means that the air flow can be simply multiplied by the number of the fans when there is no resistance. However, the maximum static pressure stays the same regardless the number of the fans. Thus, if there is large resistance, the air flow will increase very little.

In contrast, in series operation, the maximum air flow stays the same regardless the number of the fans. Instead, the static pressure is increased. When two fans are in series, the static pressure is almost doubled according to RD16, or it becomes approximately 1.5 – 2 times larger depending on type of the fans according to RD17. Serial operation is suitable for a system which has large resistance.
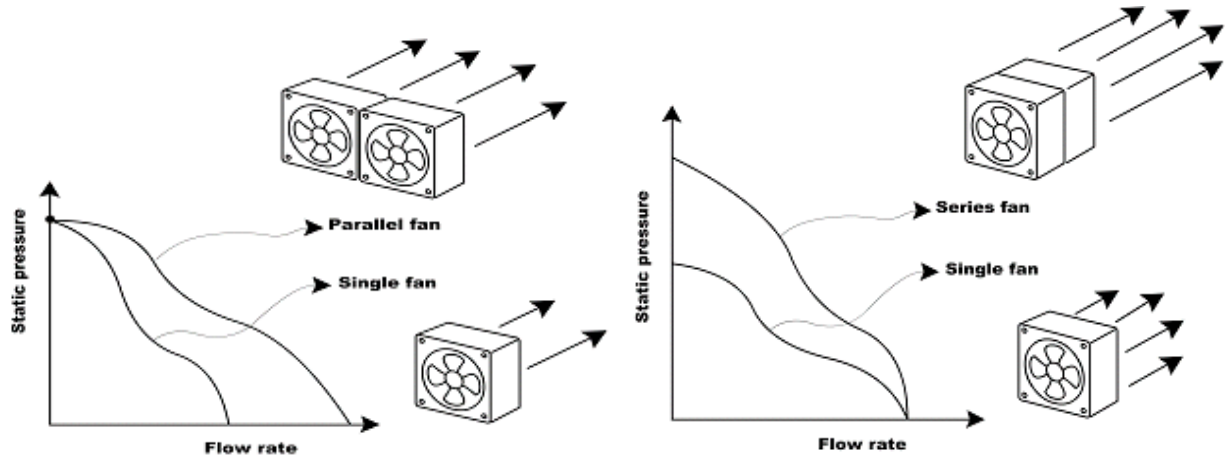
Figure 31: P-Q curve of two fans in parallel (left) and in series (right) [RD16].

Appendix D   Temperature Difference between Inlet and Outlet

Relation between the inlet and outlet air temperature of an enclosure (e.g. server chassis, room) is

$$T_o - T_i = \Delta T = \frac{q}{\rho C_p Q} \tag{32}$$

where

- T_o Outlet Air Temperature [°C]
- T_i Inlet Air Temperature [°C]
- ΔT Temperature Difference between Inlet and Outlet [°C]
- q Heat Dissipation within the Enclosure [W]
- Q Air Flow [m^3/s]
- ρ Air Density [kg/m^3]
- Cp   Specific Heat of Air [J/(kg•°C)]

Air density ρ and specific heat Cp have been discussed in Appendix A, and they can be considered as constant at a certain condition. So, this relation indicates that, regardless of inlet air temperature, the temperature difference ΔT only depnds on air flow Q and heat dissipation q. If Q and q are constant, the outlet air temperature simply increases by the same amount as the inlet air temperature.

To be exact, air density depends on temperature. However, if the temperature difference is not high like 10 ℃ at room temperature, air density difference is around 3 % (=10 / 300 K), which can be neglected in many cases. In this study, such small density difference is neglected and assumes that it is constant as discussed in Appendix A.
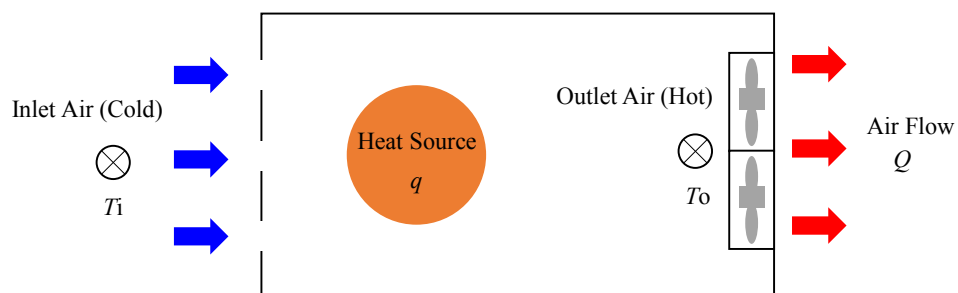
Figure 32: Tempearture difference of outlet and inlet air.